

eScholarship

Combinatorial Theory

Title

Saturation of Newton polytopes of type A and D cluster variables

Permalink

<https://escholarship.org/uc/item/7x0979ct>

Journal

Combinatorial Theory, 2(2)

ISSN

2766-1334

Authors

Mattoo, Amal

Sherman-Bennett, Melissa

Publication Date

2022

DOI

10.5070/C62257869

Supplemental Material

<https://escholarship.org/uc/item/7x0979ct#supplemental>

Copyright Information

Copyright 2022 by the author(s). This work is made available under the terms of a Creative Commons Attribution License, available at

<https://creativecommons.org/licenses/by/4.0/>

Peer reviewed

SATURATION OF NEWTON POLYTOPES OF TYPE A AND D CLUSTER VARIABLES

Amal Mattoo^{*1} and Melissa Sherman-Bennett^{†2}

¹*Department of Mathematics, Columbia University, U.S.A.*

amal.mattoo@columbia.edu

²*Department of Mathematics, University of Michigan, Ann Arbor, U.S.A.*

msherben@umich.edu

Submitted: Oct 19, 2021; Accepted: May 5, 2022; Published: Jun 30, 2022

© The authors. Released under the CC BY license (International 4.0).

Abstract. We study Newton polytopes for cluster variables in cluster algebras $\mathcal{A}(\Sigma)$ of types A and D. A famous property of cluster algebras is the Laurent phenomenon: each cluster variable can be written as a Laurent polynomial in the cluster variables of the initial seed Σ . The cluster variable Newton polytopes are the Newton polytopes of these Laurent polynomials. We show that if Σ has principal coefficients or boundary frozen variables, then all cluster variable Newton polytopes are saturated. We also characterize when these Newton polytopes are *empty*; that is, when they have no non-vertex lattice points.

Keywords. Cluster algebras, Newton polytopes, snake graphs

Mathematics Subject Classifications. 13F60, 52B20

1. Introduction

Cluster algebras are a class of commutative rings with a rich combinatorial structure, introduced by Fomin and Zelevinsky [FZ02]. A cluster algebra of rank n includes two sets of distinguished elements which together generate the algebra: a finite set of *frozen variables* and a (usually infinite) set of *cluster variables*. Cluster variables are grouped together in overlapping n -subsets, called *clusters*. A cluster together with the frozen variables is a *seed*¹. The frozen variables, their inverses, and the cluster variables generate \mathcal{A} as an algebra. A key feature of cluster algebras is the *Laurent phenomenon*: each cluster variable can be written as a Laurent polynomial in the variables of any cluster [FZ02].

^{*}Supported by the Herchel Smith–Harvard Undergraduate Science Research Program at Harvard University.

[†]Supported by NSF Graduate Research Fellowship No. DGE-1752814.

¹Technically, a seed additionally includes a rectangular extended exchange matrix; this will not matter for our purposes, as the cluster determines the seed for these cluster algebras [FZ03].

Here, we study Newton polytopes of Laurent polynomial expressions for cluster variables (or, briefly, “cluster variable Newton polytopes”).

Definition 1.1. Given a Laurent polynomial

$$f(x_1, \dots, x_d) = \sum_{\mathbf{a} \in \mathbb{Z}^d} c_{\mathbf{a}} x_1^{a_1} \cdots x_d^{a_d}$$

the *support* of f is $\{\mathbf{a} \in \mathbb{Z}^d : c_{\mathbf{a}} \neq 0\}$. The Newton polytope of f , denoted $N(f)$, is the convex hull of its support. A Newton polytope $N(f)$ is *saturated* if every lattice point of $N(f)$ is in the support of f , and $N(f)$ is *empty* if every lattice point of $N(f)$ is a vertex².

Note that emptiness is strictly stronger than saturation. Both conditions, roughly, ensure that not too much information is lost in passing from f to $N(f)$. See [MTY19] for a survey of saturated Newton polytopes in algebraic combinatorics. Empty polytopes have been studied in e.g. [BK00, DO95, Kan99]; examples include matroid polytopes (more generally, any polytope whose vertices are 0–1 vectors) and Delaunay polytopes.

We will focus particularly on cluster variable Newton polytopes for type A and D cluster algebras. Such cluster algebras are *finite type*, meaning that they have only finitely many cluster variables [FZ03]; they are also examples of cluster algebras from surfaces [FST08]. We study three different choices of frozen variables: no frozen variables, *principal coefficients* (see [FZ07]), and *boundary冻子* (where frozen variables correspond to the boundary segments of the relevant surface).

Newton polytopes of cluster variables, and more generally the support of cluster variables, have been used to construct bases for cluster algebras in the rank 2 case. Sherman and Zelevinsky gave an explicit description of all Newton polytopes in rank 2 cluster algebras of finite and affine type, and used the Newton polytopes to construct canonical \mathbb{Z} -bases [SZ04]. Their approach inspired the definition of greedy bases for arbitrary rank 2 cluster algebras in [LLZ14]. Greedy basis elements are uniquely characterized (up to scalar multiples) by a condition on their supports.

While the greedy basis has not been defined for higher rank, one might hope to find similar support characterizations for other bases for cluster algebras. This is one motivation for studying Newton polytopes of cluster variables. Many known bases of cluster algebras include the cluster variables, so understanding the support of cluster variables is a first step toward understanding supports of arbitrary basis elements. Newton polytopes of cluster variables also feature centrally in positive tropicalizations of finite type cluster algebras [AHHL20, JLS20, SW05]: the positive tropicalization is the normal fan of the Minkowski sum of all cluster variable Newton polytopes.

Other work on cluster variable Newton polytopes includes [LLS20], where Newton polytopes for rank 3 cluster algebras with no frozen variables were computed. They are weakly convex quadrilaterals that may or may not be saturated. Cluster variable Newton polytopes for cluster algebras with principal coefficients were studied by Fei in [Fei19], under the guise of F -polynomial Newton polytopes. Fei used representation theoretic methods to show principal

²A polytope which intersects a lattice exactly in its vertex set is sometimes also called “lattice-free”.

coefficient cluster variable Newton polytopes are saturated when the initial seed is acyclic³. He further conjectured that saturation holds in general.

Conjecture 1.2 ([Fei19, Conjecture 5.3]). Let $\mathcal{A}(\Sigma)$ be a cluster algebra with principal coefficients at the seed Σ . Then the Newton polytopes of cluster variables, written as Laurent polynomials in Σ , are saturated.

Here, we prove Fei's conjecture in types A and D for an arbitrary choice of initial seed Σ . Note that, as mentioned above, saturation for acyclic Σ was previously proved by Fei; our proofs do not depend on his work, and we give independent, non-representation theoretic proofs for this case⁴. We also prove saturation for other choices of frozen variables.

Theorem 1.3. *The Newton polytope of an arbitrary cluster variable in $\mathcal{A}(\Sigma)$ (written as a Laurent polynomial in Σ) is saturated when $\mathcal{A}(\Sigma)$ is one of the following cluster algebras:*

1. *type A with boundary frozen variables at Σ (Theorem 4.2)*
2. *type A with principal coefficients at Σ (Theorem 4.7)*
3. *type A with no frozen variables (Theorem 4.10)*
4. *type D with boundary frozen variables at Σ (Theorem 5.10)*
5. *type D with principal coefficients at Σ (Theorem 5.18).*

We also investigate the emptiness of cluster variable Newton polytopes. One inspiration for this is work of Kalman [Kal13], who studied cluster variable Newton polytopes for type A cluster algebras with boundary frozen variables. Among other things, he showed that each vector in the support of the cluster variable is a vertex of the Newton polytope. He further conjectured that the Newton polytope has no lattice points in its relative interior.

We prove something stronger than Kalman's conjecture: we show that the Newton polytope is in fact empty. More generally, we characterize when cluster variable Newton polytopes are empty for the cluster algebras listed in Theorem 1.3. This characterization is easiest to state in type A .

Theorem 1.4. *Let $\mathcal{A}(\Sigma)$ be a type A cluster algebra with boundary冻 or principal coefficients at Σ . Then all cluster variable Newton polytopes are empty (Theorem 4.2 and Theorem 4.7).*

We characterize emptiness in the type A no frozen variable case in Corollary 4.11; in the type D boundary frozen variable case in Theorem 5.16; and in the type D principal coefficients case in Theorem 5.20. In these cases, only some cluster variable Newton polytopes are empty; roughly speaking, these cluster variables are far away from the initial seed.

³Cluster variable Newton polytopes for principal coefficient cluster algebras are related to those for cluster algebras with arbitrary frozen variables by a linear map given by the columns of the extended exchange matrix. However, this map is not usually unimodular, so may not preserve saturation.

⁴After this manuscript appeared, Fei's conjecture was proven in full generality in [LP22].

We also give examples of non-saturated cluster variable Newton polytopes for other surface-type cluster algebras with boundary coefficients (Section 6). However, we do not find any counterexamples to Conjecture 1.2.

Our proofs of both saturation and emptiness results are inductive and involve a careful analysis of the combinatorics of snake graphs, which give Laurent polynomial formulas for cluster variables in surface-type cluster algebras [MSW11]. Though we deal with the simplest of surface-type cluster algebras, the required analysis in type D is quite delicate and not at all trivial. In particular, our proofs crucially rely on the fact that there is an upper bound on the number of times two arcs in a polygon or punctured polygon cross. This is not true for arbitrary surfaces, which is the main obstacle in using our techniques to prove Conjecture 1.2.

The paper is organized as follows. Section 2 contains background information on cluster algebras of types A and D . We also recall the results of [MSW11] on formulas for Laurent polynomial expressions for cluster variables using matchings of “snake graphs” (following [MSW11]). Section 3 introduces a number of polytopes of interest, and we prove some relevant lemmas. In Section 4, we prove saturation and emptiness results for type A cluster algebras with boundary frozen variables, principal coefficients, and no frozen variables. In Section 5, we prove saturation and emptiness results for type D cluster algebras with boundary frozen variables and principal coefficients. Finally, in Section 6 we present examples of un-saturated cluster variable Newton polytopes for other surface-type cluster algebras from boundary coefficients, showing that many of our results are unlikely to extend to general surfaces. Nonetheless, we give a few conjectures about saturation for cluster algebras from surfaces.

2. Background

Cluster algebras of finite type (that is, with finitely many cluster variables) were classified in [FZ03]; their classification matches that of finite type Dynkin diagrams. We will focus exclusively on cluster algebras of types A and D . In general, a cluster algebra \mathcal{A} is defined recursively from an initial seed Σ using a local move called *mutation*. We will take a shortcut: for our cluster algebras of interest, rather than define mutation, we will provide explicit Laurent polynomial formulas for the cluster variables of \mathcal{A} in terms of Σ . Choosing a different initial seed will result in different Laurent polynomial formulas.

As we will recall below, for type A and D cluster algebras, the combinatorics of clusters and cluster variables are encapsulated by triangulations of certain marked surfaces. We consider three different choices of frozen variables: no frozen variables; *boundary frozen variables*, which correspond to the boundary segments of the surface; and *principal coefficients* at the initial seed Σ (see [FZ07]). We first review the combinatorial objects indexing seeds and cluster variables, and then, for each choice of frozen variables, give Laurent polynomial formulas for cluster variables.

2.1. Tagged arcs and triangulations of polygons and punctured polygons

For type A and D cluster algebras, cluster variables and extended clusters are in bijection with the tagged arcs and triangulations, respectively, of two particular marked surfaces.

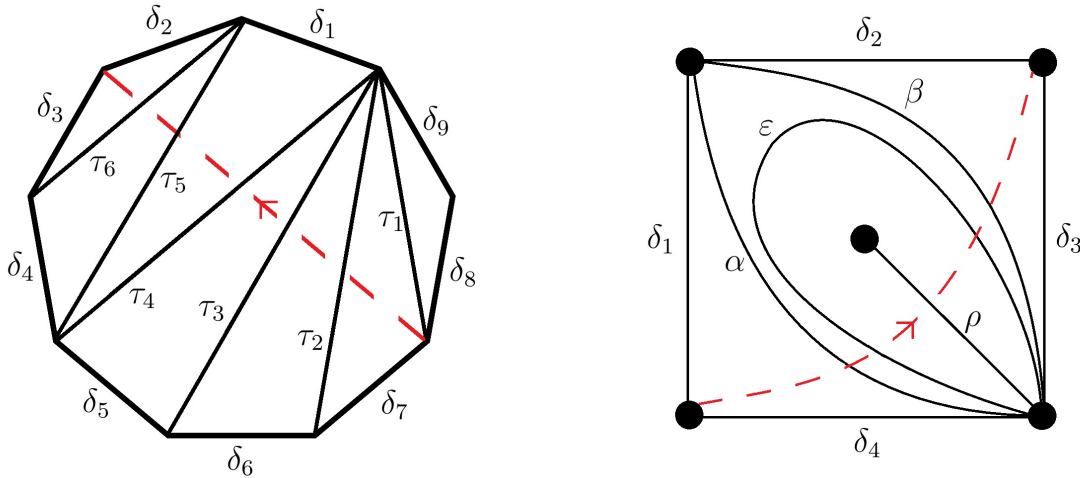


Figure 2.1: An ideal triangulation of a polygon (left) and a punctured polygon (right) and an arc, shown in red/dashed. Note that the triangulation of the punctured polygon includes a loop enclosing a radius.

Definition 2.1. Let S be a connected oriented surface with boundary (possibly empty), and let $M \subset S$ be a finite set of points with at least one on each boundary component. The elements of M are *marked points*, elements of M in the interior of S are *punctures*, and (S, M) is a *marked surface*.

For a type A cluster algebra, the relevant marked surface \mathbf{P} is a polygon whose marked points are the vertices. For a type D cluster algebra, the relevant marked surface \mathbf{P}^* is a polygon whose marked points are the vertices and a single puncture.

Definition 2.2. An (*ordinary*) *arc* in a marked surface (S, M) is a curve $\gamma \subset S$, considered up to isotopy, with endpoints in M such that: other than its endpoints, γ is disjoint from M and ∂S ; γ does not intersect itself except possibly at endpoints; and γ does not, by itself or together with a segment of the boundary, enclose an unpunctured monogon or unpunctured bigon.

An arc of \mathbf{P}^* is a *radius* if one endpoint is the puncture, and is a *loop* if its endpoints coincide. For \mathbf{P} , arcs are just diagonals between two non-adjacent vertices.

Definition 2.3. Two ordinary arcs in (S, M) are *compatible* if they (are isotopy equivalent to curves that) do not intersect except potentially at their endpoints. An *ideal triangulation* of (S, M) is a maximal collection of pairwise compatible arcs. The arcs of an ideal triangulation cut (S, M) into *ideal triangles*.

An ideal triangulation of \mathbf{P} is just a usual triangulation, and each ideal triangle has three distinct sides. An ideal triangulation of \mathbf{P}^* may include a *self-folded triangle*, which is a loop enclosing a radius (see Figure 2.1 for an example).

To obtain indexing sets for cluster variables and clusters, we need a generalization of arcs and ideal triangulations involving tagging.

Definition 2.4. Let (S, M) be \mathbf{P} or \mathbf{P}^\bullet . A *tagged arc* γ in (S, M) is either an ordinary arc with distinct endpoints (which we say is tagged *plain*) or a radius which is tagged *notched*. We write ρ^\bowtie for the notched version of the radius ρ . We denote by γ° the ordinary arc obtained by ignoring the tagging of γ .

Definition 2.5. Tagged arcs α and β are *compatible* if α° and β° are compatible as ordinary arcs (α° and β° may coincide) and if $\alpha^\circ, \beta^\circ$ are distinct radii, then α and β have the same tagging. A *tagged triangulation* is a maximal collection of pairwise compatible tagged arcs.

Note that for \mathbf{P} , tagged arcs and ordinary arcs coincide, so tagged triangulations are the same as usual triangulations. In a tagged triangulation of \mathbf{P}^\bullet , either all radii have the same tagging or there are exactly two tagged radii, which are ρ and ρ^\bowtie .

The following result shows how tagged arcs and triangulations relate to cluster variables and seeds.

Theorem 2.6. [FST08] Let \mathcal{A} be a cluster algebra of type A (resp. D) with frozen variables F . Then the cluster variables of \mathcal{A} are in bijection with tagged arcs of \mathbf{P} (resp. \mathbf{P}^\bullet). Writing x_τ for the cluster variable corresponding to arc τ , the map

$$T \mapsto \Sigma_T := \{x_\tau\}_{\tau \in T} \cup F$$

is a bijection between tagged triangulations of \mathbf{P} (resp. \mathbf{P}^\bullet) and seeds of \mathcal{A} .

Given T a tagged triangulation of \mathbf{P} (resp. \mathbf{P}^\bullet), we will use the following notation:

- $\mathcal{A}^{\text{bd}}(T)$ is the cluster algebra of type A (resp. D) with boundary frozen variables at the seed Σ_T . The frozen variables are in bijection with the boundary arcs of the surface⁵.
- $\mathcal{A}^{\text{pc}}(T)$ is the cluster algebra of type A (resp. D) with principal coefficients at the seed Σ_T [FZ07, Definition 3.1]. There is one frozen variable for each arc of T .
- $\mathcal{A}^{\text{nf}}(T)$, which has no frozen variables.

Next, we introduce notation for the Laurent polynomial expressions for cluster variables in these cluster algebras.

Definition 2.7. Let (S, M) be \mathbf{P} (resp. \mathbf{P}^\bullet), with boundary segments $Z = \{\zeta_1, \dots, \zeta_r\}$, let $T = \{\tau_1, \dots, \tau_n\}$ be a tagged triangulation, and let γ be a tagged arc.

- For $\mathcal{A}^{\text{bd}}(T)$, denote by $L_{T,\gamma}^{\text{bd}} := L_{T,\gamma}^{\text{bd}}(x_{\tau_1}, \dots, x_{\tau_n}, x_{\zeta_1}, \dots, x_{\zeta_r})$ the Laurent polynomial expansion for cluster variable x_γ in Σ_T .
- For $\mathcal{A}^{\text{pc}}(T)$, denote by $L_{T,\gamma}^{\text{pc}} := L_{T,\gamma}^{\text{pc}}(w_{\tau_1}, \dots, w_{\tau_n}, y_{\tau_1}, \dots, y_{\tau_n})$ the Laurent polynomial expansion for cluster variable w_γ in Σ_T . Note that w_{τ_i} is a cluster variable and y_{τ_i} is a frozen variable.
- For $\mathcal{A}^{\text{nf}}(T)$, denote by $L_{T,\gamma}^{\text{nf}} := L_{T,\gamma}^{\text{nf}}(z_{\tau_1}, \dots, z_{\tau_n})$ the Laurent polynomial expansion for cluster variable z_γ in Σ_T .

We use $L_{T,\gamma}$ to denote the Laurent polynomial without specifying the choice of frozen variables.

⁵More precisely, the exchange matrix of Σ_T has columns indexed by T and rows indexed by T and the boundary arcs. The entries reflect adjacency of arcs, and are computed according to [FST08, Definition 3.10].

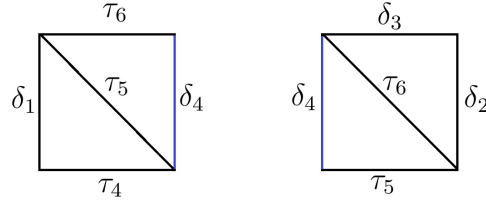


Figure 2.2: The tiles G_{τ_5} and G_{τ_6} for the triangulation T on the left of Figure 2.1. They will be glued together along the blue arcs, both of which have label δ_4 , yielding the last two boxes of the snake graph in Figure 2.4 on the left.

For every tagged triangulation T and tagged arc γ , [MSW11] gives a formula for $L_{T,\gamma}$ using matchings of snake graphs. We now review their constructions, beginning with snake graphs.

2.2. Snake graphs

Fix a surface (S, M) with boundary segments $Z = \{\zeta_1, \dots, \zeta_r\}$, and an ideal triangulation $T = \{\tau_1, \dots, \tau_n\}$. For each choice of arc γ in (S, M) , we will build a graph consisting of glued-together squares which “snakes” weakly north-west in the plane. We first define the basic building blocks of this graph.

For an ideal triangle A of $S \setminus T$ which is not self-folded, define Δ to be the triangle graph with edges labeled by the three distinct arcs of T bounding A . If A is self-folded, then define Δ to be the triangle graph with one edge labeled by the loop λ bounding A and the other two edges labeled by the radius enclosed by λ .

For $\tau \in T$, τ is in the boundary of two ideal triangles A_1 and A_2 . The *tile* G_τ is obtained by gluing together Δ_1 and Δ_2 along the edge labeled τ so that the orientations of Δ_1 and Δ_2 either both agree or both disagree with those of A_1 and A_2 (see Figure 2.2). This gives two possible planar embeddings of G_τ . If τ is a radius enclosed in a loop λ , then $A_1 = A_2$ and we glue Δ_1 and Δ_2 so that the edges labeled λ are adjacent.

Now, let $\gamma \notin T$ be an ordinary arc in (S, M) and choose an orientation of γ . Let $\tau_{i_1}, \dots, \tau_{i_k}$ (not necessarily distinct) be the sequence of arcs of T that γ intersects, and set $G_j := G_{\tau_{i_j}}$. We construct the *snake graph* $G_{T,\gamma}$ as follows. Choose the planar embedding of G_1 so that the orientation of its triangles agrees with those in T . For $j = 2, \dots, k$, glue G_j to G_{j-1} along the edge with the shared label so that odd tiles have triangles oriented the same as in T , and even tiles have triangles oriented oppositely (see Figure 2.2). This gluing is unambiguous except when τ_{i_j} is a radius enclosed in a loop λ ; in this case, glue G_{j-1}, G_j, G_{j+1} as illustrated in Figure 2.3. Then remove the diagonal from each tile to yield the snake graph $G_{T,\gamma}$ (see Figure 2.4).

We call G_τ with its diagonal removed a *square* or a *tile* of $G_{T,\gamma}$. For an edge e of $G_{T,\gamma}$, we denote its label by $\ell(e)$, and for a tile G_τ let $\ell(G_\tau) := \tau$.

Remark 2.8. Abusing notation, we will also use the term *snake graph* to refer to an edge-labeled graph G which is isomorphic to some $G_{T,\gamma}$ as an unlabeled graph. Again, for e an edge of G , we use $\ell(e)$ to denote its label.

We are interested in weight vectors of perfect matchings of $G_{T,\gamma}$. There will be three different

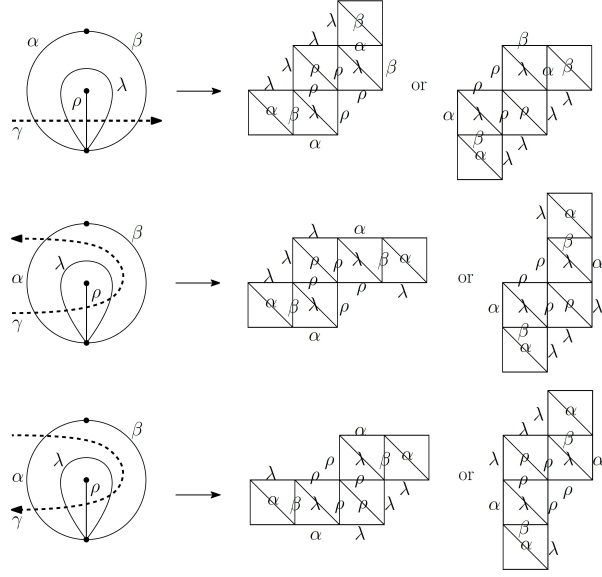


Figure 2.3: How to glue tiles $G_\lambda, G_\rho, G_\lambda$ when γ crosses a self-folded triangle. Note that if T contains a loop λ , then λ is enclosed in a bigon, as pictured here. The snake graphs on the left show the case when G_λ is oriented as in T ; on the right, the case when G_λ has the opposite orientation.

kinds of weight vectors, one for each choice of frozen variables. We first need some preliminary definitions.

Definition 2.9. A *perfect matching* M of a graph G is a subset of edges such that each vertex of G is in exactly one edge of M . The *bottom matching* M_0 of a snake graph G is the matching which only involves boundary edges of G and contains the south edge of the first tile.

See Figure 2.5 for an example.

Lemma 2.10. [MSW11, Lemma 4.7] For any matching M of $G_{T,\gamma}$, the symmetric difference $M \ominus M_0$ encloses a set of tiles of $G_{T,\gamma}$.

For a matching M of $G_{T,\gamma}$, let $C(M)$ denote the set of tiles enclosed by $M \ominus M_0$ (see Figure 2.5).

Definition 2.11. Let $G_{T,\gamma}$ be a snake graph and let M be a perfect matching. We define the following *weights* of M :

$$\begin{aligned} \text{wt}^{\text{bd}}(M) &:= \prod_{e \in M} x_{\ell(e)} \\ \text{wt}^{\text{nf}}(M) &:= \prod_{e \in M} z_{\ell(e)}|_{z_{\zeta_i}=1} \\ \text{wt}^{\text{pc}}(M) &:= \prod_{e \in M} w_{\ell(e)}|_{w_{\zeta_i}=1} \prod_{s \in C(M)} y_{\ell(s)} \end{aligned}$$

with $\text{wt}(M)$ denoting the weight when the choice of frozen variables has not been specified.

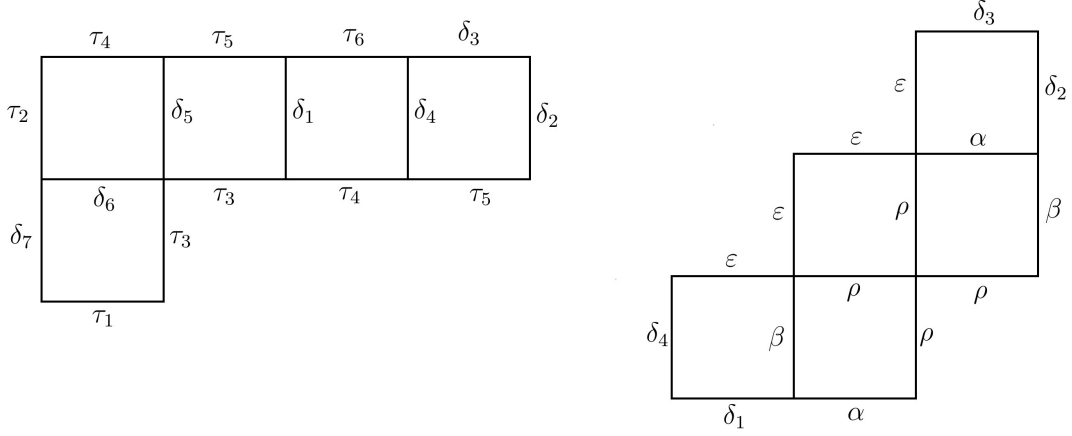
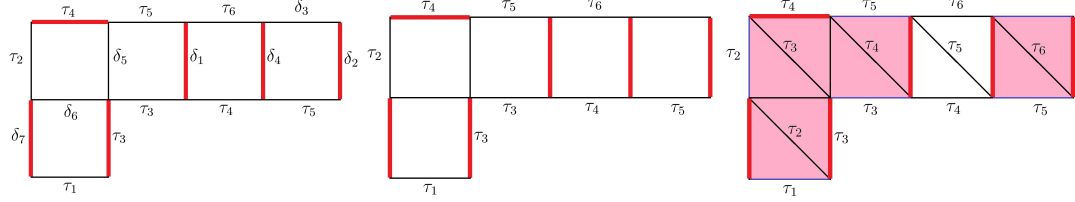


Figure 2.4: Snake graphs corresponding to the red arcs and triangulations in Figure 2.1, with the snake graph corresponding to the polygon on the left and the punctured polygon on the right.



$$\text{wt}^{\text{bd}}(M) = x_{\tau_3} x_{\tau_4} x_{\delta_1} x_{\delta_2} x_{\delta_4} x_{\delta_7} \quad \text{wt}^{\text{nf}}(M) = z_{\tau_3} z_{\tau_4} \quad \text{wt}^{\text{pc}}(M) = w_{\tau_3} w_{\tau_4} y_{\tau_2} y_{\tau_3} y_{\tau_4} y_{\tau_6}$$

$$w_{\text{bd}}^M = (0, 0, 1, 1, 0, 0; 1, 1, 0, 1, 0, 0, 1, 0, 0) \quad w_{\text{nf}}^M = (0, 0, 1, 1, 0, 0) \quad w_{\text{pc}}^M = (0, 0, 1, 1, 0, 0; 0, 1, 1, 1, 0, 1)$$

Figure 2.5: A matching M (in thickened red) of the snake graph from Figure 2.4 on the left, and the weights and weight vectors for the three choices of frozen variables. On the far right, the bottom matching is in blue, and the squares in $C(M)$ are highlighted in pink.

We denote the exponent vectors of these weights by

$$\begin{aligned} w_{\text{bd}}^M &\in \mathbb{R}^{\tau_1, \dots, \tau_n, \zeta_1, \dots, \zeta_r} \\ w_{\text{nf}}^M &\in \mathbb{R}^{\tau_1, \dots, \tau_n} \\ w_{\text{pc}}^M &\in \mathbb{R}^{\tau_1, \dots, \tau_n} \times \mathbb{R}^{\tau_1, \dots, \tau_n} \end{aligned}$$

respectively, and call them the *weight vectors* of M .

We define weights and weight vectors of matchings analogously for snake graphs H which are subgraphs of $G_{T,\gamma}$. See Figure 2.5 for examples of weights and weight vectors.

We will need the following notion in our proofs.

Definition 2.12. Let G be a snake graph. A *corner square* of G is a square (not the first or last) whose neighboring squares share a vertex with each other. All other squares are *non-corner squares*.

2.3. Expansion formulas

In this section, we give the formulas of [MSW11] for $L_{T,\gamma}$ using matchings of snake graphs. First, we note that it suffices to provide $L_{T,\gamma}$ for tagged triangulations T with no notched radii.

Proposition 2.13. [MSW11, Proposition 3.16] *Let $T = (\tau_1, \dots, \tau_n)$ be a tagged triangulation of \mathbf{P}^\bullet or \mathbf{P} and γ a tagged arc. Let γ^p be the arc obtained from γ by changing the tagging if γ° is a radius; otherwise, set $\gamma^p = \gamma$. Let $T^p := (\tau_1^p, \dots, \tau_n^p)$. Then*

$$L_{T,\gamma}^{\text{bd}} = L_{T^p, \gamma^p}^{\text{bd}}|_{x_{\tau^p} \mapsto x_\tau}, \quad L_{T,\gamma}^{\text{nf}} = L_{T^p, \gamma^p}^{\text{nf}}|_{z_{\tau^p} \mapsto z_\tau}, \quad L_{T,\gamma}^{\text{pc}} = L_{T^p, \gamma^p}^{\text{pc}}|_{w_{\tau^p} \mapsto w_\tau, y_{\tau^p} \mapsto y_\tau} \quad (2.1)$$

Because of Proposition 2.13, we will restrict our attention to tagged triangulations T of the following kind.

Definition 2.14. Let T° be an ideal triangulation of \mathbf{P}^\bullet or \mathbf{P} . We define the *corresponding tagged triangulation* T as follows. If T° has no loops, let T be the tagged triangulation with the same arcs, all tagged plain. If T° has a loop λ enclosing a radius ρ , then let T be the tagged triangulation replacing λ with ρ^\bowtie and all other arcs the same as in T° . We say that tagged triangulations arising in this way *correspond to an ideal triangulation*.

Remark 2.15. If T is a tagged triangulation of \mathbf{P}^\bullet that does not correspond to an ideal triangulation, then T has all radii notched. This means T^p does correspond to an ideal triangulation. By Proposition 2.13, each $L_{T,\gamma}$ can be obtained from L_{γ^p, T^p} by a simple change of variables. Thus, we need only provide formulas for $L_{T,\gamma}$ where T corresponds to an ideal triangulation.

Note that all tagged triangulations of \mathbf{P} correspond to ideal triangulations.

2.3.1 Expansion formulas for plain arcs

We now have all of the ingredients to give $L_{T,\gamma}$ for γ a plain tagged arc and T a tagged triangulation corresponding to an ideal triangulation.

In what follows, if λ is a loop enclosing a radius ρ , we set $x_\lambda := x_\rho x_{\rho^\bowtie}$. We also set $L_{T,\lambda} := L_{T,\rho} L_{T,\rho^\bowtie}$.

Theorem 2.16. [MSW11, Theorem 4.10] *Let (S, M) be a polygon or punctured polygon with boundary segments $\{\zeta_1, \dots, \zeta_r\}$, and let $T^\circ = \{\tau_1, \dots, \tau_n\}$ be an ideal triangulation with corresponding tagged triangulation T . Consider an oriented ordinary arc γ (which may be a loop), and let $\tau_{i_1}, \dots, \tau_{i_d}$ be the sequence of arcs γ intersects in T° . Then*

$$\begin{aligned} L_{T,\gamma}^{\text{bd}} &= \frac{1}{x_{\tau_{i_1}} \dots x_{\tau_{i_d}}} \sum_M \text{wt}^{\text{bd}}(M), \\ L_{T,\gamma}^{\text{pc}} &= \frac{1}{w_{\tau_{i_1}} \dots w_{\tau_{i_d}}} \sum_M \text{wt}^{\text{pc}}(M), \\ L_{T,\gamma}^{\text{nf}} &= \frac{1}{z_{\tau_{i_1}} \dots z_{\tau_{i_d}}} \sum_M \text{wt}^{\text{nf}}(M) \end{aligned} \quad (2.2)$$

where the sum is over perfect matchings M of the snake graph $G_{T^\circ, \gamma}$.

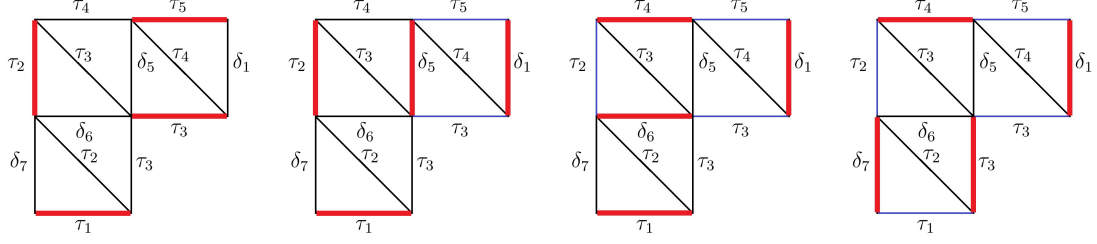


Figure 2.6: All matchings of a snake graph $G_{T,\gamma}$ (red), with edges of the bottom matching in blue.

Note that Theorem 2.16 gives expansion formulas for all cluster variables in a type A cluster algebra.

Remark 2.17. There are two situations in which Theorem 2.16 gives L_{T,ρ^\bowtie} for a notched radius ρ . The first: if $T = T^p$, then L_{T,ρ^\bowtie} for any radius ρ can be obtained from $L_{T,\rho}$ using Proposition 2.13. The second: if $\rho \in T$, then let λ be the loop enclosing ρ . Then $L_{T,\lambda} = L_{T,\rho} L_{T,\rho^\bowtie}$, and since $L_{T,\rho} = x_\rho$ (resp. w_ρ or z_ρ) is a cluster variable by assumption we have $L_{T,\rho^\bowtie} = (1/x_\rho)L_{T,\lambda}$ (resp. w_ρ or z_ρ).

Example 2.18. For γ and T with $G_{T,\gamma}$ as in Figure 2.6, we have the following expansion formulas (note how each term corresponds to a matching):

$$L_{T,\gamma}^{\text{bd}} = \frac{x_{\tau_1}x_{\tau_2}x_{\tau_3}x_{\tau_5} + x_{\tau_1}x_{\tau_2}x_{\delta_1}x_{\delta_5} + x_{\tau_1}x_{\tau_4}x_{\delta_1}x_{\delta_6} + x_{\tau_3}x_{\tau_4}x_{\delta_1}x_{\delta_7}}{x_{\tau_2}x_{\tau_3}x_{\tau_4}}$$

$$L_{T,\gamma}^{\text{nf}} = \frac{z_{\tau_1}z_{\tau_2}z_{\tau_3}z_{\tau_5} + z_{\tau_1}z_{\tau_2} + z_{\tau_1}z_{\tau_4} + z_{\tau_3}z_{\tau_4}}{z_{\tau_2}z_{\tau_3}z_{\tau_4}}$$

$$L_{T,\gamma}^{\text{pc}} = \frac{w_{\tau_1}w_{\tau_2}w_{\tau_3}w_{\tau_5} + w_{\tau_1}w_{\tau_2}y_{\tau_4} + w_{\tau_1}w_{\tau_4}y_{\tau_3}y_{\tau_4} + w_{\tau_3}w_{\tau_4}y_{\tau_2}y_{\tau_3}y_{\tau_4}}{w_{\tau_2}w_{\tau_3}w_{\tau_4}}.$$

2.3.2 Expansion formulas for notched arcs

Now we consider expansion formulas for x_{ρ^\bowtie} (resp. w_{ρ^\bowtie} or z_{ρ^\bowtie}), for ρ a radius. They are of a similar flavor, but involve ρ -symmetric matchings of snake graphs.

Fix $T^\circ = \{\tau_1, \dots, \tau_n\}$ an ideal triangulation of \mathbf{P}^\bullet and let T be the corresponding tagged triangulation. We may assume that $\rho \notin T$ and that $T \neq T^p$ (see Remark 2.17), so in fact $T = T^\circ$. Let λ be the loop enclosing ρ .

Definition 2.19. The snake graph $G_{T,\lambda}$ contains two disjoint subgraphs isomorphic to $G_{T,\rho}$ as labeled graphs, one on each end. We denote these graphs by $G_{T,\rho,1}$ and $G_{T,\rho,2}$. Let $H_{T,\rho,i}$ be the subgraph of $G_{T,\rho,i}$ obtained by deleting edges labeled by radii. (See Figure 2.7)

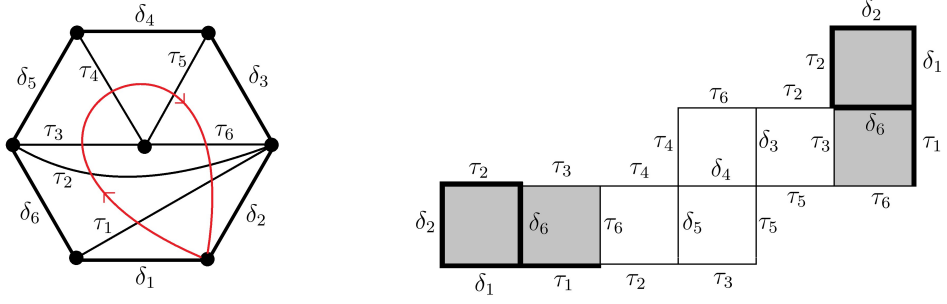


Figure 2.7: An example of $G_{T,\lambda}$ for λ a loop (shown in red). The squares of the subgraphs $G_{T,\rho,i}$ are shaded; the edges of $H_{T,\rho,i}$ are in bold.

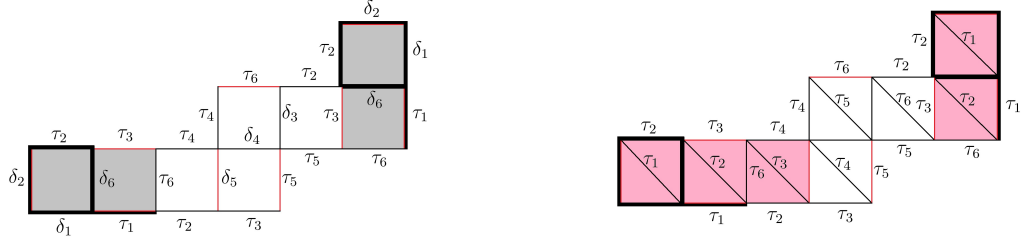


Figure 2.8: A ρ -symmetric matching M (red) of snake graph $G_{T,\lambda}$ from Figure 2.7 with boundary frozen variables, and of the corresponding snake graph with principal coefficients. The pink squares correspond to $C(M)$. The edges of M are labeled, in counter-clockwise order starting from the bottom-left end: $\delta_2, \tau_1, \delta_5, \tau_5, \tau_3, \tau_1, \delta_2, \tau_6, \tau_3$.

Definition 2.20. A perfect matching M of $G_{T,\lambda}$ is ρ -symmetric if $M|_{H_{T,\rho,1}} \cong M|_{H_{T,\rho,2}}$. The weight of a ρ -symmetric matching M is given by

$$\overline{\text{wt}}(M) := \frac{\text{wt}(M)}{\text{wt}(M|_{G_{T,\rho,i}})}$$

where i is chosen so that $M|_{G_{T,\rho,i}}$ is a perfect matching of $G_{T,\rho,i}$ (such an i exists by [MSW11, Lemma 12.4]).

The weight vector of a ρ -symmetric matching is the exponent vector of its weight.

Example 2.21. For the matching M in Figure 2.8, we have the weights:

$$\begin{aligned} \overline{\text{wt}}^{\text{bd}}(M) &= \frac{x_{\tau_1}^2 x_{\tau_3}^2 x_{\tau_5} x_{\tau_6} x_{\delta_2}^2 x_{\delta_5}}{x_{\tau_1} x_{\tau_3} x_{\delta_2}} = x_{\tau_1} x_{\tau_3} x_{\tau_5} x_{\tau_6} x_{\delta_2} x_{\delta_5} \\ \overline{\text{wt}}^{\text{pc}}(M) &= \frac{w_{\tau_1}^2 w_{\tau_3}^2 w_{\tau_5} w_{\tau_6} y_{\tau_1}^2 y_{\tau_2}^2 y_{\tau_3}}{w_{\tau_1} w_{\tau_3} y_{\tau_1} y_{\tau_2}} = w_{\tau_1} w_{\tau_3} w_{\tau_5} w_{\tau_6} y_{\tau_1} y_{\tau_2} y_{\tau_3} \end{aligned}$$

Theorem 2.22. [MSW11, Theorem 4.17] Let $T = \{\tau_1, \dots, \tau_n\}$ be a tagged triangulation of \mathbf{P}^\bullet which is also an ideal triangulation. Suppose $\rho \notin T$ is a radius, and let λ be the loop enclosing ρ . Let $\tau_{i_1}, \dots, \tau_{i_k}$ be the sequence of arcs of T that λ intersects, and suppose ρ intersects $\tau_{i_1}, \dots, \tau_{i_d}$. Then

- $L_{T,\rho^\bowtie}^{\text{bd}} = \frac{1}{x_{\tau_{i_{d+1}}} \cdots x_{\tau_{i_k}}} \sum_M \overline{\text{wt}}^{\text{bd}}(M)$
- $L_{T,\rho^\bowtie}^{\text{pc}} = \frac{1}{w_{\tau_{i_{d+1}}} \cdots w_{\tau_{i_k}}} \sum_M \overline{\text{wt}}^{\text{pc}}(M)$
- $L_{T,\rho^\bowtie}^{\text{nf}} = \frac{1}{z_{\tau_{i_{d+1}}} \cdots z_{\tau_{i_k}}} \sum_M \overline{\text{wt}}^{\text{nf}}(M)$

where the sum is over ρ -symmetric matchings of $G_{T,\lambda}$.

3. Newton polytopes and perfect matching polytopes

In this section, we define perfect matching polytopes and give their relation to the Newton polytopes $N(L_{T,\gamma}) \subset \mathbb{R}^T$.

To simplify notation, set $N(T, \gamma) := N(L_{T,\gamma})$, with $N^{\text{bd}}(T, \gamma)$, $N^{\text{pc}}(T, \gamma)$, and $N^{\text{nf}}(T, \gamma)$ defined accordingly.

Remark 3.1. Proposition 2.13, particularly the substitution in (2.1), implies that $N(T, \gamma)$ and $N(T^p, \gamma^p)$ differ only by renaming coordinates. Thus, when proving the saturation of $N(T, \gamma)$, we may assume the tagged triangulation T corresponds to an ideal triangulation. We will make this assumption for the remainder of the paper.

Recall the definition of weight vector w^M of a perfect matching M (see Definition 2.11).

Definition 3.2. Given a snake graph $G_{T,\gamma}$, the *perfect matching polytope* $P(G)$ is the convex hull of $\{w^M : M \text{ is a perfect matching of } G\}$. We say that the perfect matching polytope $P(G)$ is *saturated* if every lattice point in $P(G)$ is the weight vector of a matching, and we say it is *empty* if every lattice point in $P(G)$ is a vertex.

Note that $P^{\text{bd}}(G)$, $P^{\text{pc}}(G)$, and $P^{\text{nf}}(G)$ are defined using w_{bd}^M , w_{pc}^M , and w_{nf}^M respectively. Each polytope lies in the vector space containing the corresponding weight vectors, as given in Definition 2.11.

Definition 3.3. Let $G_{T,\gamma}$ be a snake graph, and let G' be a snake graph identical to G but with edges given unique labels. The *lifted perfect matching polytope* $\overline{P}(G)$ is the convex hull of the indicator vectors $\chi_M \in \mathbb{R}^{E(G)}$, where M ranges over all perfect matchings of G' .

Similarly, the *lifted principal perfect matching polytope* $\overline{P}^{\text{pc}}(G)$ is the convex hull of the indicator vectors $(\chi_M, \chi_{C(M)}) \in \mathbb{R}^{E(G)} \times \mathbb{R}^{S(G)}$, where $S(G)$ is the set of squares of G' and M ranges over all perfect matchings of G' .

The polytope $\overline{P}(G)$ is frequently called the perfect matching polytope; we depart from this because of our interest in graphs with non-distinct edge labels.

The following lemma explains our interest in perfect matching polytopes.

Lemma 3.4. Let $T^\circ = \{\tau_1, \dots, \tau_n\}$ be an ideal triangulation of \mathbf{P} or \mathbf{P}^\bullet , and let T be the corresponding tagged triangulation. Let γ be an ordinary arc (including possibly a loop). Then $N(T, \gamma)$ is saturated (resp. empty) if and only if $P(G_{T^\circ, \gamma})$ is saturated (resp. empty).

Proof. We use notation for \mathcal{A}^{bd} , as the proofs for the other two are identical.

There are two cases. If $T^\circ = T$ (i.e. T° has no loops), then by Theorem 2.16, the set of weight vectors $W := \{w^M : M \text{ is a perfect matching of } G_{T^\circ, \gamma}\}$ differs from the support of $L_{T, \gamma}$ by an element of \mathbb{Z}^T . So $P(G_{T^\circ, \gamma})$ is an integer translate of $N(T, \gamma)$.

If $T^\circ \neq T$, then T° contains a loop λ enclosing a radius ρ . The tagged triangulation T contains ρ^\bowtie and not λ , and in (2.2), we set $x_\lambda = x_\rho x_{\rho^\bowtie}$ to obtain a term of $L_{T, \gamma}$ from the weight of a matching of $G_{T^\circ, \gamma}$.

Consider the map $\xi : \mathbb{R}^{T^\circ} \mapsto \mathbb{R}^T$, which fixes coordinates indexed by $T^\circ \cap T$ and sends the others to

$$\begin{aligned}\xi(v)_\rho &= v_\lambda + v_\rho \\ \xi(v)_{\rho^\bowtie} &= v_\lambda.\end{aligned}$$

Theorem 2.16 implies that there exists $\eta \in \mathbb{Z}^T$ such that $\xi(W) + \eta$ is the support of $L_{T, \gamma}$. In particular, $\xi(P(G_{T^\circ, \gamma})) + \eta$ is equal to $N(T, \gamma)$. Since ξ and translation by η are both bijective on lattice points, the statement follows. \square

The lifted (principal) perfect matching polytopes are our main tool to prove saturation of perfect matching polytopes. The lifted matching polytopes are combinatorially easy to understand. We then carefully analyze the effects of projecting the lifted matching polytopes to the matching polytopes, using the following natural projection.

Let $G = G_{T, \gamma}$ and let Z denote as usual the boundary arcs of the surface (S, M) . We have projection maps

$$\pi^{\text{bd}} : \mathbb{R}^{E(G)} \rightarrow \mathbb{R}^T \times \mathbb{R}^Z \tag{3.1}$$

$$\pi^{\text{nf}} : \mathbb{R}^{E(G)} \rightarrow \mathbb{R}^T \tag{3.2}$$

$$\pi^{\text{pc}} : \mathbb{R}^{E(G) \times S(G)} \rightarrow \mathbb{R}^T \times \mathbb{R}^T \tag{3.3}$$

given by summing coordinates according to the labels of the indexing edge or square. For example, the τ_j th coordinate of $\pi^{\text{bd}}(v)$ is

$$\sum_{\substack{e \in E(G): \\ \ell(e) = \tau_j}} v_e.$$

We will simply write π if we do not want to specify the vector spaces, or if it is clear from context.

Note that π is a surjection from incidence vectors of $\overline{P}(G)$ (resp. $\overline{P}^{\text{pc}}(G)$) to weight vectors of $P^{\text{bd}}(G)$ and $P^{\text{nf}}(G)$ (resp. $P^{\text{pc}}(G)$).

The lifted perfect matching polytopes have a straightforward description.

Proposition 3.5. ([Edm65], see also [LP86, Theorem 7.3.4]) *Let G be a snake graph. Then*

$$\overline{P}(G) = \{w \in \mathbb{R}^{E(G)} : w_e \geq 0, \sum_{e \ni v} w_e = 1 \text{ for all } v \in G\}.$$

Corollary 3.6. *Let G be a snake graph. Then for each $s \in S(G)$, there is some $e_s \in E(G)$ an edge of s , and a map f_s , which is either $x \mapsto x$ or $x \mapsto 1 - x$, such that*

$$\begin{aligned} \overline{P}^{\text{pc}}(G) = \{ (w_1, w_2) \in \mathbb{R}^{E(G)} \times \mathbb{R}^{S(G)} : (w_1)_e \geq 0, (w_2)_s = f_s((w_1)_{e_s}), \\ \sum_{e \ni v} (w_1)_e = 1 \text{ for all } v \in G \} \end{aligned}$$

Proof. Each square $s \in S(G)$ has an edge e_s on the boundary of G . If $e_s \notin M_0$, then for any matching M we have $e_s \in M$ if and only if $s \in C(M)$; if $e_s \in M_0$, then for any matching M we have $e_s \in M$ if and only if $s \notin C(M)$. In the former case, let $f_s : x \mapsto x$ and in the latter case let $f_s = x \mapsto 1 - x$. If $(w_1, w_2) = \chi(M)$ is a principal incidence vector for a matching M , then we have $(w_2)_s = f_s((w_1)_{e_s})$. The same relation must hold in any element of the convex hull of the incidence vectors. The relations given in Lemma 3.5 must also hold. And since we have a (coordinate) projection $\overline{P}^{\text{pc}}(G) \rightarrow \overline{P}(G)$, the dimension of the former must be at least that of the latter, so there cannot be any additional relations. \square

The preceding proof shows that we have an affine map $\alpha : \overline{P}(G) \rightarrow \overline{P}^{\text{pc}}(G)$, which is inverse to the natural projection $\overline{P}^{\text{pc}}(G) \rightarrow \overline{P}(G)$. Coordinate-wise, α is defined by $(\alpha(v)_1)_e = v_e$ and $(\alpha(v)_2)_s = f_s(v_s)$.

Next, we show that lifted matching polytopes have the nice properties we care about.

Lemma 3.7. *Let G be a snake graph. Then $\overline{P}(G)$ and $\overline{P}^{\text{pc}}(G)$ are empty and, in particular, are saturated.*

Proof. By Lemma 3.5, each lattice point η in $\overline{P}(G)$ has $\eta_e = 0$ or $\eta_e = 1$. Further, for each vertex v of G , there is exactly one edge e containing v such that $\eta_e = 1$. Thus, each lattice point is the weight vector of a perfect matching for G .

Note that all weight vectors are 0/1 vectors with $|E(G)|/2$ coordinates equal to 1. This implies that a nontrivial convex combination of weight vectors is not a weight vector, so all weight vectors are vertices of $\overline{P}(G)$.

Since the affine isomorphism between $\overline{P}(G)$ and $\overline{P}^{\text{pc}}(G)$ in the proof of Corollary 3.6 maps lattice points to lattice points, the desired statement holds for $\overline{P}^{\text{pc}}(G)$ as well. \square

Remark 3.8. By Lemma 3.7, a lattice point $v \in P(G)$ is a weight vector if and only if $\pi^{-1}(v) \subset \overline{P}(G)$ (resp. $\overline{P}^{\text{pc}}(G)$) contains a lattice point. This will be our general strategy for proving saturation of $P(G)$. For emptiness, we will consider collections of weight vectors such that some convex combination of them is equal to a lattice point, and then show that at most one vector in the combination has a positive coefficient.

4. Type A cluster variable Newton polytopes

Here we restrict our attention to cluster variables of cluster algebras of type A ; that is, to triangulations T and arcs γ of a polygon \mathbf{P} .

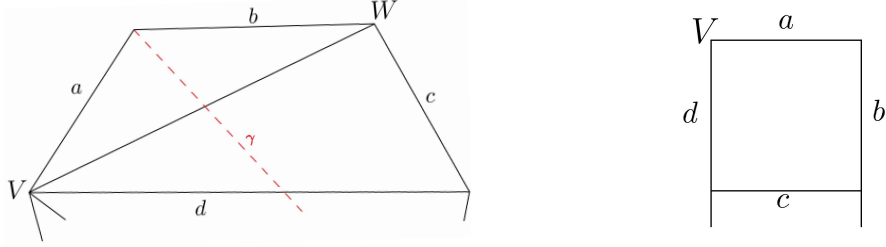


Figure 4.1: On the left, the final quadrilateral of T crossed by arc γ . On the right, the final square of $G_{T,\gamma}$.

4.1. Boundary frozen variables

We first show that the projection map π^{bd} is very well-behaved on $\overline{P}(G_{T,\gamma})$. For the rest of this section, let $\pi = \pi^{\text{bd}}$ and $P(G) = P^{\text{bd}}(G)$.

Lemma 4.1. *Let T be a triangulation of \mathbf{P} and let γ be an arc. For v a lattice point of $P(G_{T,\gamma})$, $\pi^{-1}(v) \subseteq \mathbb{Z}^{E(G_{T,\gamma})}$.*

Proof. We will employ induction on the number of squares in $G_{T,\gamma}$. If there is exactly one square, then all edges will have different labels, so π is the identity map.

If $G_{T,\gamma}$ has more than one square, assume the lemma holds for all smaller snake graphs, and suppose for the sake of contradiction that there exists a non-lattice point $\bar{v} \in \overline{P}(G_{T,\gamma})$ such that $\pi(\bar{v}) \in P(G_{T,\gamma})$ is a lattice point. Let the boundary segments and arcs of T around one endpoint of γ be as shown in Figure 4.1 on the left, so the final tile of $G_{T,\gamma}$ is as in Figure 4.1 on the right. Let γ' be the arc obtained by changing the endpoint of γ to vertex W in Figure 4.1 on the left, so $G_{T,\gamma'}$ is equal to $G_{T,\gamma}$ with the last square removed. Note that a, b, c each appear only once as edge labels of $G_{T,\gamma}$, so $\bar{v}_a, \bar{v}_b, \bar{v}_c \in \{0, 1\}$. And $\bar{v}_a + \bar{v}_d = 1$, so $\bar{v}_d \in \{0, 1\}$ too.

If $\bar{v}_a = 1$, then $\bar{v}_b = \bar{v}_d = 0$, so some other coordinate of \bar{v} must be a non-integer. Deleting coordinates $\bar{v}_a, \bar{v}_b, \bar{v}_d$ yields a non-lattice point \bar{v}' in $\overline{P}(G_{T,\gamma'})$ with $\pi(\bar{v}') \in P(G_{T,\gamma'})$ a lattice point, contradicting the inductive hypothesis. If instead $\bar{v}_a = 0$, define \bar{v}' by $\bar{v}'_c = \bar{v}'_a = 1, \bar{v}'_b = \bar{v}'_d = 0$ and all other coordinates equal to those of \bar{v} ; deleting coordinates $\bar{v}'_a, \bar{v}'_b, \bar{v}'_d$ yields a non-lattice point of $\overline{P}(G_{T,\gamma'})$ similarly contradicting the inductive hypothesis. \square

Now we can prove our first main result.

Theorem 4.2. *Let \mathcal{A}^{bd} be a type A cluster algebra with boundary coefficients. Then the Newton polytope of any cluster variable, written as a Laurent polynomial in an arbitrary seed, is saturated and empty.*

Proof. Let T be a triangulation of \mathbf{P} and γ an arc. By Lemma 3.4, $N^{\text{bd}}(T, \gamma)$ is saturated if and only if $P(G_{T,\gamma})$ is saturated. By Lemma 4.1, every lattice point v in $P(G_{T,\gamma})$ has an integer point $\bar{v} \in \pi^{-1}(v)$. By Remark 3.8, this implies $P(G_{T,\gamma})$ is saturated.

Lemma 4.1 and Lemma 3.7 together imply that each lattice point of $P(G_{T,\gamma})$ is the image under π of a vertex of $\overline{P}(G_{T,\gamma})$. By [Kal13, proof of Theorem 4.13], π maps vertices of $\overline{P}(G_{T,\gamma})$

to vertices of $P(G_{T,\gamma})$.⁶ □

Remark 4.3. Note the key properties of triangulations of \mathbf{P} we used in Lemma 4.1: that each quadrilateral in a triangulation involves four distinct arcs, and that there are strict limits on the number of times each edge label occurs in $G_{T,\gamma}$. The former will fail for punctured surfaces, where we encounter self-folded triangles, and the latter will fail for surfaces with non-finite cluster type, where arcs can intersect arbitrarily many times.

4.2. Principal coefficients

For the case of type A cluster algebras with principal coefficients, we will use a similar strategy to the case of boundary frozen variables. However, the additional structure of principal coefficients will simplify our work. For this section, let $\pi = \pi^{\text{pc}}$.

Lemma 4.4. *For any arc τ_i labeling an edge in $G_{T,\gamma}$, one of the following is true for all $\bar{v} = (\bar{v}_1, \bar{v}_2) \in \overline{P}^{\text{pc}}(G_{T,\gamma}) \subset \mathbb{R}^{E(G)} \times \mathbb{R}^{S(G)}$:*

- *There is a unique edge e in $G_{T,\gamma}$ with $\ell(e) = \tau_i$.*
- *There is $\sigma \in T$ such that $(\bar{v}_1)_{\tau_i} = (\bar{v}_2)_{\sigma}$.*
- *There is $\sigma \in T$ such that $(\bar{v}_1)_{\tau_i} = 1 - (\bar{v}_2)_{\sigma}$.*

Proof. If the first condition does not hold, then τ_i appears exactly twice in $G_{T,\gamma}$ and labels edges on the boundary of $G_{T,\gamma}$. Let σ be the label of a square in $G_{T,\gamma}$ with one of its boundary edges labeled by τ_i . Then by Corollary 3.6 and its proof, either $(\bar{v}_1)_{\tau_i} = (\bar{v}_2)_{\sigma}$ or $(\bar{v}_1)_{\tau_i} = 1 - (\bar{v}_2)_{\sigma}$. □

Lemma 4.5. $\pi : \overline{P}^{\text{pc}}(G_{T,\gamma}) \rightarrow P^{\text{pc}}(G_{T,\gamma})$ maps non-lattice points to non-lattice points.

Proof. Let \bar{v} be a point in $\overline{P}^{\text{pc}}(G_{T,\gamma})$ such that $v = \pi(\bar{v})$ is a lattice point. Since γ intersects each arc of T at most once $(v_2)_{\sigma} = (\bar{v}_2)_{\sigma} \in \{0, 1\}$ for each $\sigma \in T$. Next, for each $\tau \in T$, if there is a unique edge labeled τ then $(v_1)_{\tau} = (\bar{v}_1)_{\tau} \in \{0, 1\}$. And by Lemma 4.4, if τ is not a unique label then $(\bar{v}_1)_{\tau}$ is either $(\bar{v}_2)_{\sigma}$ or $1 - (\bar{v}_2)_{\sigma}$. Thus, all coordinates of \bar{v} are integers, proving the contrapositive of the lemma. □

We can use the reasoning of this proof to show the following relationship between polytopes.

Proposition 4.6. *There is an affine inverse $\pi^{-1} : P^{\text{pc}}(G_{T,\gamma}) \rightarrow \overline{P}^{\text{pc}}(G_{T,\gamma})$ of π . In particular, π is a combinatorial equivalence between the two polytopes.*

Proof. As we saw in the proof of Lemma 4.5, given $v = \pi(\bar{v})$, we can recover the coordinates of \bar{v} by Lemma 4.4. We saw that each coordinate of \bar{v} is either equal to a coordinate of v or equal to 1 minus a coordinate of v . Performing these coordinate-wise operations yields the desired map π^{-1} . □

⁶Note that [Kal13, Theorem 4.13] does not imply this theorem. Take P_1 to be the line segment in \mathbb{R}^2 with endpoints $(0, 0)$ and $(1, 2)$ and P_2 the line segment in \mathbb{R} with endpoints 0 and 2 . Projecting onto the 2nd coordinate takes P_1 to P_2 , with vertices going to vertices, but the lattice point $1 \in P_2$ does not have a lattice point in its preimage.

Theorem 4.7. *Let \mathcal{A}^{pc} be a type A cluster algebra with principal coefficients at a seed Σ . Then the Newton polytope of any cluster variable, written as a Laurent polynomial in Σ , is saturated and empty.*

Proof. Let T be the triangulation corresponding to Σ and choose an arc γ of \mathbf{P} . As before, it suffices to prove saturation and emptiness of $P^{\text{pc}}(G_{T,\gamma})$. By Lemma 4.5, the preimage under π of any lattice point of $P^{\text{pc}}(G_{T,\gamma})$ is a lattice point of $\overline{P}^{\text{pc}}(G_{T,\gamma})$, and by Lemma 3.7, each lattice point of $\overline{P}^{\text{pc}}(G_{T,\gamma})$ is a vertex. This shows that each lattice point of $P^{\text{pc}}(G_{T,\gamma})$ is the weight vector of a matching, proving saturation. And since π is a combinatorial equivalence by Proposition 4.6, it must map vertices to vertices, proving emptiness. \square

4.3. No frozen variables

The case of Type A cluster algebras with no frozen variables is considerably different from the previous cases. The added difficulty arises from the fact that the natural projection $\overline{P}(G) \rightarrow P^{\text{nf}}(G)$ is *not* a combinatorial isomorphism.

The following lemma restricts when non-vertex lattice points may arise.

Lemma 4.8. *Let T be a triangulation of \mathbf{P} and γ an arc. For $G = G_{T,\gamma}$, let S be a set of matchings such that $\text{Conv}_{M \in S} \{w_{\text{nf}}^M\}$ contains a non-vertex lattice point. Then for any $M_1, M_2 \in S$, the symmetric difference $M_1 \ominus M_2$ is the union of all edges of a set of pairwise-disjoint squares of G .*

Proof. Without loss of generality assume there is a lattice point $\eta = \sum_{M \in S} c_M w_{\text{nf}}^M$ such that $\sum_{M \in S} c_M = 1$ and $0 < c_M < 1$ for each c_M . For each coordinate i , either $(w_{\text{nf}}^M)_i = (w_{\text{nf}}^{M'})_i$ for all $M, M' \in S$, or there exist $M, M' \in S$ such that $(w_{\text{nf}}^M)_i = 0, (w_{\text{nf}}^{M'})_i = 2$.

Assume for the sake of contradiction that there exist $M_1, M_2 \in S$ that violate the statement of the lemma. Let α be the first square in G such that there exist $M_1, M_2 \in S$ with $(M_1 \ominus M_2)|_\alpha$ consisting of two or three edges. Noting that α cannot be the last square of G , let β be the square following α in G .

We see by induction on $|G|$ that M_1 and M_2 restricted to α and β must contain the edges shown in Figure 4.2: this is true if α is the first square in G , and otherwise M_1 and M_2 restricted to the first square both contain either the same edge or a pair of opposite edges; removing this edge or these edges we obtain a pair of perfect matchings for a smaller diagram.

In Figure 4.2, the edge e appears in one matching but not the other. And $\ell(e)$ cannot be a boundary segment unless there are exactly two squares in the diagram (in which case the lemma is vacuously true), nor does $\ell(e)$ appear again to the northwest of β . Thus, either $(w_{\text{nf}})_{\ell(e)} \in \{0, 1\}$ for all $M \in S$, or $(w_{\text{nf}})_{\ell(e)} \in \{1, 2\}$ for all $M \in S$, contradicting the hypothesis and proving the lemma. \square

In fact, we can sharpen this lemma.

Lemma 4.9. *Assuming the same hypothesis as Lemma 4.8, every matching in S must consist of a pair of opposite sides from every other square of the snake graph, starting with the first and ending with the last. Each of these pairs will be present in at least one matching of S .*

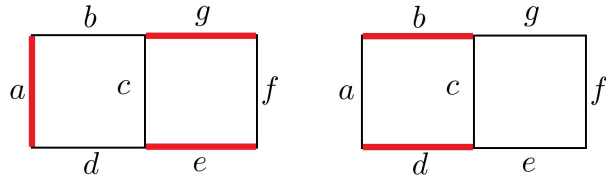


Figure 4.2: Necessary configuration for proof by contradiction in Lemma 4.8.

Proof. Let α be any square where two matchings $M_1, M_2 \in S$ differ. By Lemma 4.8, every matching in S must contain opposite sides of α . Then α cannot be the second (or second to last) square of G , or else the edge $e \in \alpha$ with $\ell(e)$ non-boundary and unique in G would have $\eta_{\ell(e)}$ between 0 and 1.

Next, assume α is not one of the first two or last squares of G , and let edges $e_1, e_2 \in \alpha$ have $\ell(e_1), \ell(e_2)$ non-boundary segments. Let α_1 be the square two before α and let α_2 be the square two after α . Let edges $e'_1 \in \alpha_1$ and $e'_2 \in \alpha_2$ have $\ell(e_1) = \ell(e'_1)$ and $\ell(e_2) = \ell(e'_2)$. Without loss of generality, $e_1, e_2 \in M_1$ and $e_1, e_2 \notin M_2$, so we must have $\{(w_{\text{nf}}^M)_{\ell(e_1)}\}_{M \in S} = \{(w_{\text{nf}}^M)_{\ell(e_2)}\}_{M \in S} = \{0, 1, 2\}$. Thus, some elements of S must differ on whether they include e'_1 and e'_2 , so every matching in S must contain opposite sides of α_1 and α_2 . Continuing recursively yields the lemma. \square

Now we can show that all non-vertex lattice points are weight vectors of matchings.

Theorem 4.10. *Let \mathcal{A}^{nf} be a cluster algebra of type A with no frozen variables. Then the Newton polytope of any cluster variable, written as a Laurent polynomial in an arbitrary seed, is saturated.*

Proof. Let T be a triangulation of \mathbf{P} and γ an arc. Again recall that by Lemma 3.4, $N^{\text{nf}}(T, \gamma)$ is saturated if and only if $P^{\text{nf}}(G_{T, \gamma})$ is saturated. Let E be the set of edges e appearing in the alternating squares described in Lemma 4.9 such that $\ell(e)$ is not a boundary segment. By that lemma, the only possible non-vertex lattice point of $P^{\text{nf}}(G)$ is η with $\eta_\tau = 1$ if there exists $e \in E$ with $\ell(e) = \tau$ and $\eta_\tau = 0$ otherwise. We can always construct M with $w_{\text{nf}}^M = \eta$ by picking a pair of opposite sides from each of the alternating squares. \square

Emptiness no longer holds in general, but Lemma 4.9 tells us exactly what non-vertex lattice points must look like.

Corollary 4.11. *Let \mathcal{A}^{nf} be a cluster algebra of type A with no frozen variables. Let T be a triangulation of \mathbf{P} and γ an arc. Then the Newton polytope of the cluster variable $L_{T, \gamma}^{\text{nf}}$ is empty if and only if at least one of the following conditions does not hold.*

- γ intersects all arcs in T .
- n is odd and at least 3.
- If γ intersects τ_1, \dots, τ_n in that order, τ_{i-1} and τ_{i+1} do not share an endpoint for even i .

Proof. Each of these conditions is necessary for the existence of $M_1, M_2 \in S$ as described in Lemma 4.9: the first ensures that interior edges of G are labeled by non-boundary segments and the latter two ensure that the alternate squares do not share a corner. And by the final construction in the proof of Lemma 4.9, if all the stated conditions hold we can construct matchings M_1 and M_2 with $w_{\text{nf}}^{M_1} \neq w_{\text{nf}}^{M_2}$ but $\frac{1}{2}w_{\text{nf}}^{M_1} + \frac{1}{2}w_{\text{nf}}^{M_2} \in \mathbb{Z}^n$. \square

Remark 4.12. We observe that the results for type A cluster algebras with no frozen variables are considerably less elegant than for our other two choices of frozen variables. Therefore, we focus on the latter two cases for type D cluster algebras. Based on experiments, we expect that the case of type D cluster algebras with no frozen variables is analogous to the type A case with no frozen variables — i.e., all Newton polytopes saturated and complicated conditions characterizing emptiness — but the proof above does not extend directly to the type D case.

5. Type D cluster variable Newton polytopes

Now we turn to cluster variables in cluster algebras of type D ; that is, to tagged arcs γ and triangulations T of \mathbf{P}^\bullet . Recall that we assume T corresponds to an ideal triangulation (see Remark 2.15).

5.1. Boundary frozen variables

We will show that $N^{\text{bd}}(T, \gamma)$ is always saturated (Theorem 5.10) considering the case of plain arcs (Proposition 5.8) and notched arcs (Lemma 5.9) separately. In type D , Lemma 4.1 no longer holds. As a result, our proofs in this section are somewhat more involved.

For this section, let $\pi = \pi^{\text{bd}}$, $P(G) = P^{\text{bd}}(G)$, and $w^M = w_{\text{bd}}^M$.

Our proof strategy is strong induction. We use the following observation in the inductive step. Recall the definition of a non-corner square of a snake graph (Definition 2.12).

Observation 5.1. *Let G be a snake graph and let H be an “initial” or “final” sub-snake graph of G which is connected to the rest of G by a non-corner square with outer edges e_1 and e_2 . The graph $K := G \setminus (H \cup \{e_1, e_2\})$ is also a snake graph, and the union of any matchings of H and K is a matching of G . If $P(K)$ is saturated, then to show a lattice point $v \in P(G)$ is the weight vector of a matching, it suffices to find $\bar{v} \in \pi^{-1}(v)$ where $\bar{v}|_{E(H)}$ gives a matching of H .*

We begin with some lemmas giving sufficient conditions for saturation of $P(G)$ in terms of saturation of $P(G')$, for G' a sub-snake graph.

Lemma 5.2. *For a snake graph G , suppose that the first tile of G has edges e_1, e_2, e_3, e_4 (clockwise) such that e_1 connects the first tile to another tile in G and the label of at least one of e_2, e_3, e_4 is unique in the diagram. Let G' be a snake graph obtained by deleting some boxes from that end of G , inheriting the edge labels of G . Then $P(G)$ will be saturated if $P(G')$ is saturated for all such G' .*

Proof. Assume saturation of all such $P(G')$, let $v \in P(G)$ be a lattice point, and let $\bar{v} \in \overline{P}(G)$ lie in $\pi^{-1}(v)$. By the given uniqueness of a label, at least one of $\bar{v}_{e_2}, \bar{v}_{e_3}, \bar{v}_{e_4}$ is 0 or 1, and so either: $\bar{v}_{e_2} = \bar{v}_{e_4} = 0$ and $\bar{v}_{e_3} = 1$, or $\bar{v}_{e_2} = \bar{v}_{e_4} = 1$ and $\bar{v}_{e_3} = 0$.

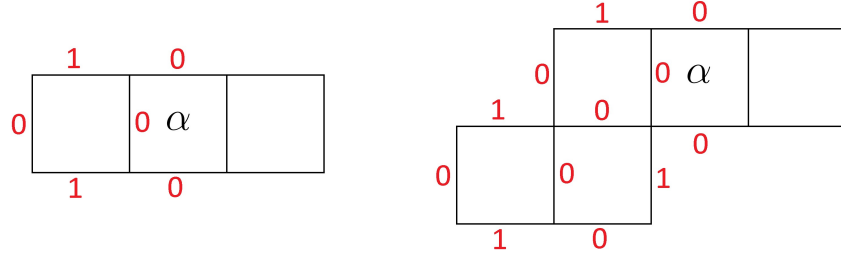


Figure 5.1: Two examples of the case of $\bar{v}_{e_2} = \bar{v}_{e_4} = 1$ in Lemma 5.2. The numbers in red are coordinates of \bar{v} . Note that up to the second non-corner square, all coordinates are determined by the fact that the sum around each vertex must be 1.

If $\bar{v}_{e_2} = \bar{v}_{e_4} = 0$, we are in the scenario of Observation 5.1, where H is e_3 and K is the graph obtained from G by deleting e_2, e_3, e_4 ($P(K)$ is saturated by assumption). So using Observation 5.1, we can find a matching M of G with weight vector v .

Next, consider the latter case of $\bar{v}_{e_2} = \bar{v}_{e_4} = 1$. Let H be the sub-snake graph of G which is the union of tiles from the first tile up to (but not including) the next non-corner tile, which we call α . Each of the coordinates of \bar{v} corresponding to edges of H must be 0 or 1 (see Figure 5.1). Further, the coordinates indexed by the border edges of α must be 0. Again, we are in the scenario of Observation 5.1, and so can find a matching with weight vector v . \square

Lemma 5.3. *For a snake graph G , suppose the first two boxes at either end of G are as shown in Figure 5.2, where $\ell(e_i) = \ell(e'_i)$. Suppose further that $\ell(e_5)$ and one of $\ell(e_2), \ell(e_3), \ell(e_4)$ occur exactly twice in the diagram. Let G' be a snake graph obtained by deleting one or more boxes from either end of G . Then $P(G)$ is saturated if $P(G')$ is saturated for all such G' .*

Proof. Assume saturation of all such $P(G')$, let $v \in P(G)$ be a lattice point, and let $\bar{v} \in \bar{P}(G)$ lie in $\pi^{-1}(v)$. Let $e_i \in \{e_2, e_3, e_4\}$ have the edge label that occurs exactly twice, so $\bar{v}_{e_i} + \bar{v}_{e'_i} \in \{0, 1, 2\}$. If this sum is 0 or 2 then \bar{v}_{e_i} is 0 or 1 respectively, and the remainder of the proof is exactly like the proof of Lemma 5.2. Otherwise, $\bar{v}_{e_j} = 1 - \bar{v}_{e'_j}$ for $j \in \{2, 3, 4\}$. Let $x := \bar{v}_{e_2}$ and note $x = \bar{v}_{e_4} = 1 - \bar{v}_{e_3}$.

Since the label of e_5 occurs exactly twice, we similarly have $\bar{v}_{e_5} + \bar{v}_{e'_5} \in \{0, 1, 2\}$. If it is 2, then $\bar{v}_{e_5} = 1$, so $x = 0$, and we can again proceed by Observation 5.1. If it $\bar{v}_{e_5} + \bar{v}_{e'_5} = 0$, then $\bar{v}_{e_5} = \bar{v}_{e'_5} = 0$, so $\bar{v}_{e_1} = 1 - x = 1 - \bar{v}_{e'_1}$. Define $\bar{q} \in \pi^{-1}(v)$ by $\bar{q}_{e_1} = \bar{q}_{e_3} = \bar{q}_{e'_2} = \bar{q}_{e'_4} = 1$, $\bar{q}_{e'_1} = \bar{q}_{e'_3} = \bar{q}_{e_2} = \bar{q}_{e_4} = 0$, and $\bar{q}_{e_i} = \bar{v}_{e_i}$ for all other coordinates. Since $\bar{q}_{e_2} = \bar{q}_{e_4} = 0$ we can proceed by Observation 5.1, where H is e_3 .

Finally, suppose $\bar{v}_{e_5} + \bar{v}_{e'_5} = 1$ and let $\bar{v}_{e_5} = y$. We see that $x + y = 1$ so $\bar{v}_{e_1} = \bar{v}_{e'_1} = 0$ and $\bar{v}_{e_5} = y = 1 - x$. Now, let G' be G with the first and last box removed. Define $\bar{v}' \in \bar{P}(G')$ by $\bar{v}'_{e_1} = x$, $\bar{v}'_{e'_1} = 1 - x$, and $\bar{v}'_{e_i} = \bar{v}_{e_i}$ for all other coordinates. Since $P(G')$ is saturated by assumption, there is some lattice point $\bar{q}' \in \bar{P}(G')$ such that $\pi(\bar{v}') = \pi(\bar{q}')$. Without loss of generality let $\bar{q}'_{e_5} = 0$ and $\bar{q}'_{e'_5} = 1$, so $\bar{q}'_{e_1} = 1$ and $\bar{q}'_{e'_1} = 0$. Define the lattice point $\bar{q} \in \bar{P}(G)$ by $\bar{q}_{e_1} = \bar{q}_{e_3} = \bar{q}_{e'_2} = \bar{q}_{e'_4} = 0$ and $\bar{q}_{e'_3} = \bar{q}_{e_2} = \bar{q}_{e_4} = 1$ and $\bar{q}_{e_i} = \bar{q}'_{e_i}$ for all other coordinates. Then, $\pi(\bar{q}) = \pi(\bar{v}) = v$, proving saturation of G . \square

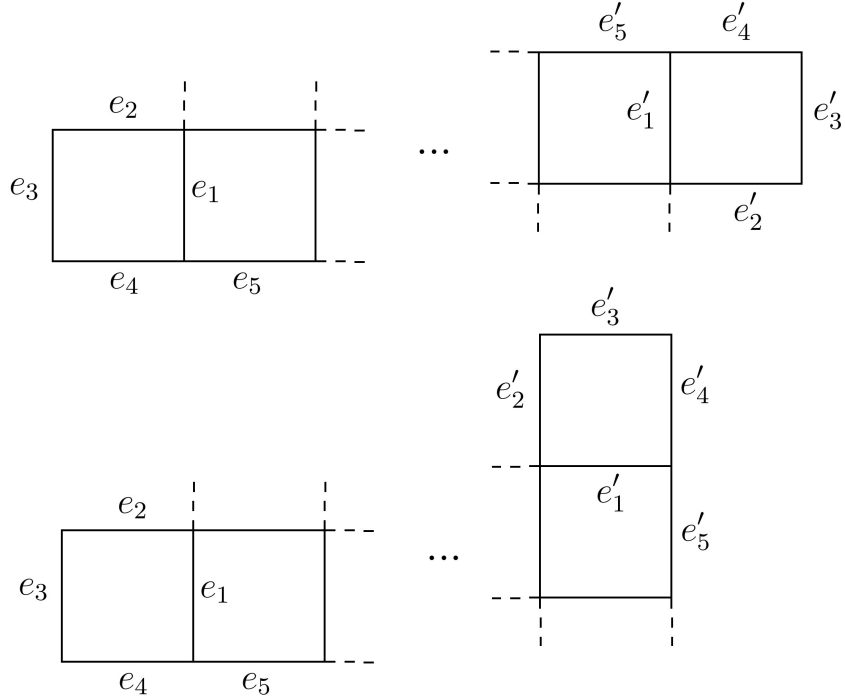


Figure 5.2: Ends of a snake graph satisfying the symmetry condition in the hypothesis of Lemma 5.3.

Now, in order to make use of the previous lemmas, we must verify which snake graphs $G_{T,\gamma}$ satisfy the hypotheses. First, we analyze the structure of ideal triangulations of \mathbf{P}^\bullet .

Fixing a triangulation T , let ρ_1, \dots, ρ_k be the radii, ordered counterclockwise, and let b_i be the basepoint of ρ_i . Note T contains an edge ε_i between each b_i and b_{i+1} , or else the space between ρ_i and ρ_{i+1} would not be triangulated. Note that $\varepsilon_1, \dots, \varepsilon_k$ form the boundary of a punctured k -gon triangulated by radii. Let B_i be the set of boundary vertices between b_i and b_{i+1} inclusive. Since no edge of T can cross one of the radii, two boundary vertices can be connected by an edge of T only if they are both in B_i . For $k > 1$, let S_i be the surface enclosed by ε_i and boundary edges between b_i and b_{i+1} . Note that S_i is isotopic to an un-punctured convex polygon and $T|_{S_i}$ is a triangulation. Thus, for $k > 1$, T is combinatorially equivalent to a punctured k -gon triangulated by k radii, with a triangulated polygon glued to each boundary segment. See Figure 5.3 for examples.

Let γ be an oriented arc not in T . We will describe its intersections with the edges of T . If γ is a radius oriented from base point V to the puncture, it will only intersect edges in some S_i followed by ε_i ; denote the ordered set of these edges by I_V . If the endpoints of γ are boundary vertices W, W' with $W \in B_i, W' \in B_j$ (possibly the same), then either γ will be a diagonal of a polygon, or it will intersect T at I_W , followed by the radii ρ_i through ρ_{j-1} ,⁷ followed by $I_{W'}$ in reverse order. Which of these two cases applies depends on which side of the puncture γ lies.

If $k > 1$ and γ intersects some ε_i twice, the first and last radius in T that γ intersects will

⁷Note that this is slightly imprecise if W or W' is in $\{b_i\}_{i=1}^k$ since i and j can be either of two values.

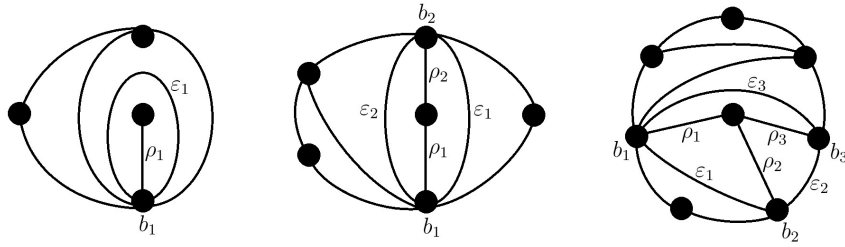


Figure 5.3: Examples of our notation for triangulations of punctured polygons with $k = 1$, $k = 2$, and $k = 3$ radii.

both correspond to non-corner squares of $G_{T,\gamma}$. This is true since γ will consecutively intersect $\varepsilon_i, \rho_i, \rho_{i-1}$ which do not share a common endpoint, and similarly on the other side. Furthermore, all other radii in T which γ intersects will correspond to corner squares, since those arcs share a common endpoint at the puncture.

Next, we use our analysis above to develop some results about edges with unique (or almost unique) labels.

Proposition 5.4. *Let T be an ideal triangulation of P^\bullet , and let γ be an arc that is either not a loop or is a loop enclosing a radius in T . Then there is at least one edge on the boundary of the initial or final box of $G_{T,\gamma}$ whose label is unique in $G_{T,\gamma}$.*

Proof. Let the end points of γ be W and W' , and let ρ_V be the radius based at V (not necessarily in T). We prove each of five cases separately.

1. There is no i with $W, W' \in B_i$, and at least one of $W, W' \notin \{b_i\}_{i=1}^k$.

Assuming W is a boundary vertex, each of the two arcs or boundary segments incident to W surrounding γ will label unique edges of $G_{T,\gamma}$ due to the type A structure near the end points. Note that this includes the case where W' is the puncture.

2. Both $W, W' \in \{b_i\}_{i=1}^k$.

The subset of T that contributes to $G_{T,\gamma}$ is isotopic to a (un-punctured) triangulated polygon, so the two arcs incident to W (resp. W') and surrounding γ will label unique edges.

3. $W, W' \in B_i$ and γ does not intersect ε_i .

In this case γ is contained in S_i , which is equivalent to an arc in an un-punctured polygon, so again the arcs incident to W, W' and surrounding γ will label unique edges.

4. $W, W' \in B_i$ and γ intersects ε_i .

Without loss of generality, $W \notin \{b_i\}_{i=1}^k$ so the arcs surrounding γ incident to W are between elements of B_i . These will not be edge labels of tiles corresponding to radii, so it suffices to consider tiles corresponding to edges in I_W and $I_{W'}$. Let $T' \subset T$ consist of arcs labeling edges of G_{T,ρ_W} . If ρ'_W is contained inside the bounds of T' , then the arcs surrounding γ containing W are unique labels. Otherwise, the arcs surrounding γ containing W' are unique labels.

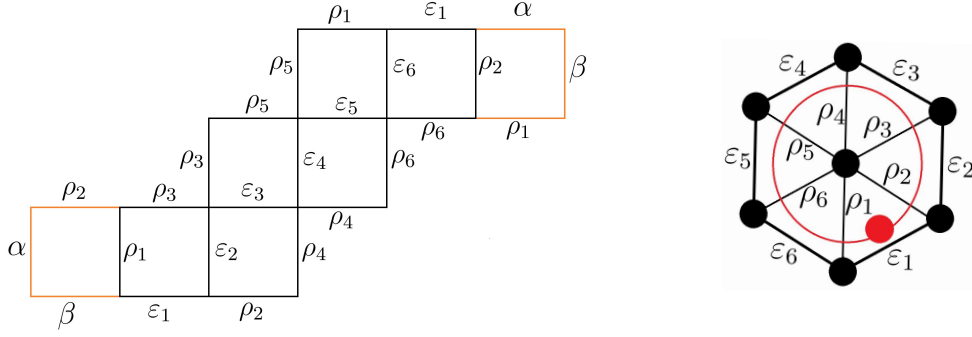


Figure 5.4: On the left is the middle part of the snake graph of a loop (with base vertex not in $\{b_i\}_{i=1}^k$) in the case $k = 6$. The tiles correspond to intersections with all radii; tiles corresponding to non-radii have been removed. On the right is a ‘floating arc’ whose intersections with the the radii would correspond to this snake graph.

5. $W = W'$

We have $W = W' = b_i$, since γ encloses a radius of T . Thus, γ is contained in the k -gon with sides $\{\varepsilon_i\}$ and intersects all radii but ρ_i . Both ε_i and ε_{i-1} label a boundary edge in an end square of $G_{T,\gamma}$, and these labels will be unique in the diagram. \square

In Lemma 5.5 and Lemma 5.6 we address two special cases where the usual induction argument cannot be applied directly.

Lemma 5.5. *Let T be an ideal triangulation of \mathbf{P}^\bullet , and let γ be a loop that intersects exactly one non-radius arc of T . Let G' be the snake graph obtained by removing the first and last square from $G_{T,\gamma}$ (as shown in Figure 5.4 when $k = 6$). Then $P(G')$ is saturated.*

Proof. If $k = 1$, then G' consists of a single box with two adjacent pairs of edges labeled ρ_1 and ε_1 respectively; $P(G')$ is a single point and so is saturated.

For $k \geq 2$, the tiles of G' alternate between horizontal and vertical adjacency, as shown in Figure 5.4.⁸ The internal edges of G' are labeled by $\varepsilon_2, \dots, \varepsilon_k$ and these labels are unique. All other labels appear exactly twice. Whenever two boundary edges meet at a vertex that is also incident to two internal edges, those two boundary edges are both labeled by ρ_i for some $i = 3, \dots, k$.

Let $\bar{v} \in \overline{P}(G')$ such that $v = \pi(\bar{v})$ is a lattice point in $P(G')$. First, consider the case $\bar{v}_{\varepsilon_i} = 0$ for all $i = 2, \dots, k$. We claim that any pair of coordinates of \bar{v} corresponding to edges with the same label must sum to 1.

To prove this claim, note that the first three external edges at each end of G' are labeled $\rho_1, \varepsilon_1, \rho_2$, and the external edges between the two ends are pairs of adjacent edges both labeled ρ_i for $2 < i \leq k$ (as seen in Figure 14). Observe that the two edges labeled ε_1 have an even number of external edges between them: edges labeled ρ_1, ρ_2 , and pairs of edges labeled ρ_i for $i > 2$. Likewise, the pairs of edges labeled ρ_1 and ρ_2 have an even number of external edges between

⁸For $k = 2$ some of the following structure degenerates, but the proof still holds.

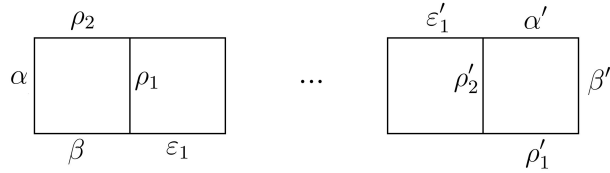


Figure 5.5: The ends of the snake graph of a loop intersecting only ε_1 and radii, in the case $k \geq 2$.

them. Thus, if a matching of G' contains only external edges, it will include one of the edges labeled ε_1 or ρ_i if and only if it does not contain the other. The claim follows.

Thus, $v_\tau = 1$ for all τ appearing more than once in G' , and v is the weight vector of either of the two perfect matchings that use only boundary edges of G' .

On the other hand, consider the case $\bar{v}_{\varepsilon_i} = 1$ for some $i \in \{2, \dots, k\}$. Then $\bar{v}_\tau = 0$ for all edges labeled τ incident to ε_i . By the equations of $\bar{P}(G')$ corresponding to degree 2 vertices of G' , we see that all coordinates of \bar{v} are either 0 or 1, meaning that \bar{v} corresponds to a perfect matching. \square

Lemma 5.6. *Let T be an ideal triangulation of \mathbf{P}^\bullet . If $\gamma \notin T$ is a loop that intersects exactly one non-radius arc of T , then $P(G_{T,\gamma})$ is saturated.*

Proof. Without loss of generality, γ intersects ε_1 , then all of $\{\rho_i\}_i$, and finally ε_1 again.

If $k = 1$, then ε_1 is a loop and $G_{T,\gamma}$ is as shown in Figure 5.8. We see saturation directly, as the only weight vectors (in the coordinates $(\alpha, \beta, \rho_1, \varepsilon_1)$) are $(2, 0, 1, 1)$, $(1, 1, 1, 1)$, $(0, 2, 1, 1)$.

For $k \geq 2$, the first two and last two squares of $G_{T,\gamma}$ are as shown in Figure 5.5, with edges differing by a prime mark labeled with the same arc. Arcs α , β , and ε_1 do not appear elsewhere in the diagram.

Let $v \in P(G_{T,\gamma})$ be a lattice point and $\bar{v} \in \pi^{-1}(v)$. We have $\bar{v}_\alpha + \bar{v}_{\alpha'} \in \{0, 1, 2\}$ and $\bar{v}_{\varepsilon_1} + \bar{v}_{\varepsilon'_1} \in \{0, 1, 2\}$, and if any of these four coordinates of \bar{v} are integers we can apply the proof of Lemma 5.3 directly after we show that $P(G')$ is saturated for all $G' \subset G$. If G' is obtained by removing one or more squares from one end of $G_{T,\gamma}$, then $P(G')$ is saturated by Lemma 5.2. If G' is obtained by removing one square from each end of $G_{T,\gamma}$, then $P(G')$ is saturated by Lemma 5.5. And if G' is obtained by removing any more squares from each end of $G_{T,\gamma}$, then $G' = G_{T,\gamma'}$ where γ' is an arc of an un-punctured polygon, so $P(G')$ is saturated by Proposition 4.2.

Now, suppose $x = 1 - \bar{v}_\alpha = \bar{v}_\beta = \bar{v}_{\rho_2} = \bar{v}_{\alpha'} = 1 - \bar{v}_{\beta'} = \bar{v}_{\rho'_1}$ and $y = \bar{v}_{\varepsilon_1} = 1 - \bar{v}_{\varepsilon'_1}$ with $0 < x, y < 1$. Since the labels $\varepsilon_2, \dots, \varepsilon_k$ that are unique in the diagram, the corresponding coordinates of \bar{v} must be integers. As in the proof of Lemma 5.5, if $\bar{v}_{\varepsilon_i} = 1$ for some i , then \bar{v}_{ε_1} and $\bar{v}_{\varepsilon'_1}$ are also integers so \bar{v} is a lattice point as desired. If instead $\bar{v}_{\varepsilon_i} = 0$ for $i = 2, \dots, k$, the equations defining $\bar{P}(G_{T,\gamma})$ imply that $v_\alpha = v_\beta = v_{\rho_i} = 1$. And this lattice point v corresponds to the matching that includes α , β' , and the bottom matching of G' , where G' is the snake graph obtained by removing the first and last squares of $G_{T,\gamma}$. \square

The next lemma will be the key ingredient of our strong induction.

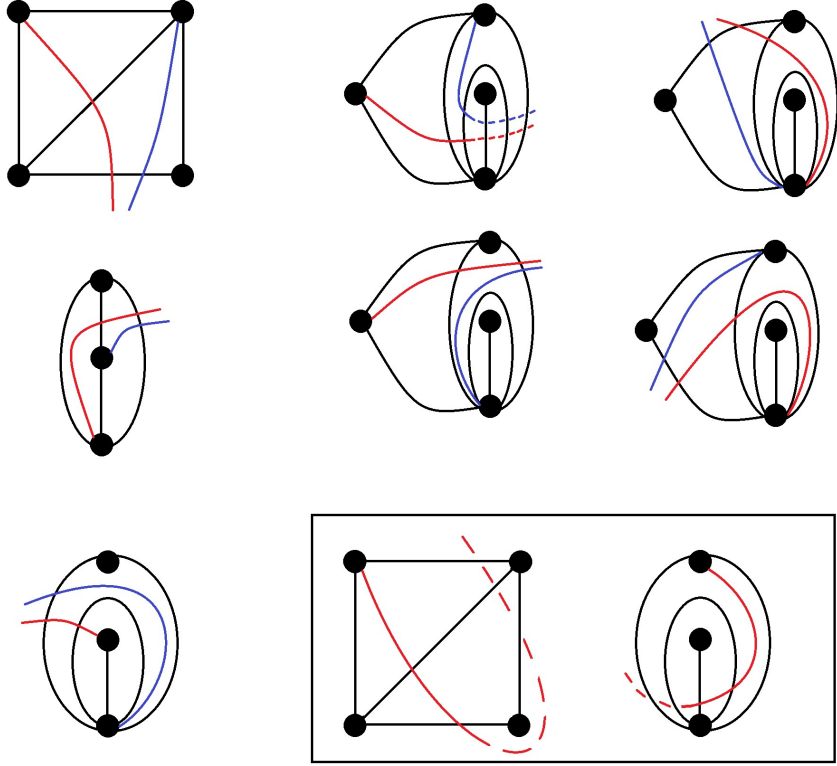


Figure 5.6: The red curves show all possible ends of arcs γ , up to symmetry, that intersect at least two edges of an ideal triangulation T . In each case, the blue curve is the end of an arc γ' such that $P(G_{T,\gamma'})$ is $P(G_{T,\gamma})$ with the last square removed from the given end. Such an arc γ' exists in all cases except one (in general as shown in the box on the left, with the case for $k = 1$ on the right).

Lemma 5.7. *Let T be an ideal triangulation of a punctured polygon and γ an arc. Let G' be any snake graph obtained by deleting at least one square from one or both ends of $G_{T,\gamma}$. Then $G' = G_{T,\gamma'}$ for some arc γ' , or $P(G')$ is saturated.*

Proof. Figure 5.6 shows how given an end of an arc γ we can find another arc γ' such that $G_{T,\gamma'}$ the graph obtained by removing one square from the appropriate end of $G_{T,\gamma}$ — in all cases but those in the box. Those cases occur if and only if the diagonal of the quadrilateral is ε_i and two of the sides are radii (the radii coincide for the case $k = 1$ shown on the right), because γ' would have to intersect itself and so wouldn't be a valid arc. For the boxed case on the left, shifting the endpoint of γ to the bottom left vertex of the quadrilateral corresponds to removing two squares from one end of $G_{T,\gamma}$ (and likewise for the $k = 1$ case by shifting the endpoint of γ to the puncture). It remains to show the following:

- If γ is a loop with both ends as in the boxed case, removing a square from each end of $G_{T,\gamma}$ yields G' with $P(G')$ saturated.
- If γ has at least one end as in the boxed case, removing one square of $G_{T,\gamma}$ from that end

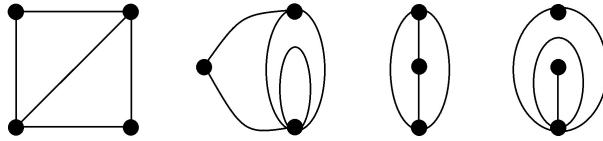


Figure 5.7: Types of quadrilaterals appearing in ideal triangulations of punctured polygons.

yields G'' with $P(G'')$ saturated.

In the first case, G' consists only of squares corresponding to radii, and Lemma 5.5 showed that $P(G')$ is saturated.

In the second case, the end of G'' contains $G_{T,\rho}$ for some radius ρ with base point at the endpoint of γ . By Proposition 5.4, at least one boundary edge of the last square of G'' is unique in the diagram, so we can use Observation 5.1 to reduce saturation of G'' to saturation of a smaller diagram, iterating until the diagram is either G' from the first case or $G_{T,\gamma'}$ for a non-loop arc γ' intersecting only radii. In the latter case, γ' is an arc of an un-punctured polygon, so $P(G_{T,\gamma'})$ is saturated by Proposition 4.2. \square

Now, we have all of the base cases and reduction techniques for a proof by induction.

Proposition 5.8. *Let T be an ideal triangulation of \mathbf{P}^\bullet , and let γ be an ordinary arc. Let T' be the corresponding tagged triangulation. Then $N(T', \gamma)$ is saturated.*

Proof. By Lemma 3.4, it suffices to show that $P(T, \gamma)$ is saturated. We proceed by induction on the number of boxes in the snake diagram $G_{T,\gamma}$. For the base case where γ intersects a single arc of T , $G_{T,\gamma}$ is a single tile and has an edge with a unique label, so $P(G_{T,\gamma})$ is saturated by Observation 5.1.

For the inductive step, assume that $P(G_{T,\gamma})$ is saturated for all $G_{T,\gamma}$ with at most t boxes. Suppose there is an arc τ such that $G_{T,\tau}$ has $t+1$ boxes. If τ is not a loop, or intersects each arc of T at most once, then Proposition 5.4, Lemma 5.7, and the inductive hypothesis ensure that the hypothesis of Lemma 5.2 is satisfied, so $P(G_{T,\tau})$ is saturated. If τ is a loop that intersects exactly one non-radius arc, then $P(G_{T,\tau})$ is saturated by Lemma 5.6. If τ is a loop that intersects at least two non-radius arcs, then by Proposition 5.4, Lemma 5.7, and the inductive hypothesis we can apply Lemma 5.3 to conclude that $P(G_{T,\tau})$ is saturated. \square

We turn to notched arcs, recalling the corresponding expansions of cluster variables are given in terms of ρ -symmetric matchings of snake graphs (see Section 2.3.2).

Proposition 5.9. *Let T be an ideal triangulation of \mathbf{P}^\bullet , and let T' be the corresponding tagged triangulation. Let ρ^\bowtie be a notched arc. Then $N(T', \rho^\bowtie)$ is saturated.*

Proof. Let λ be the loop enclosing the unnotched radius ρ . If the unnotched radius ρ is in T , then $N(T', \rho^\bowtie)$ is an integer translate of $N(T, \lambda)$ (see Remark 2.17), which is saturated by Proposition 5.8. If $T \neq T'$ (that is, if T contains a loop and $T' = (T')^p$), then $N(T', \rho^\bowtie)$ is, up to renaming coordinates, equal to $N(T', \rho)$ (see Remark 2.17). So we may assume $T = T'$ and $\rho \notin T$.

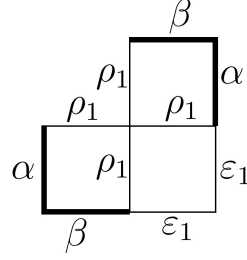


Figure 5.8: Middle part of $G_{T,\gamma}$ where γ is a loop (with base point not in $\{b_i\}$) and $k = 1$, with edges of G_1 and G_2 in bold.

Let $\{M_i\}_i$ be a set of ρ -symmetric matchings of $G_{T,\lambda}$ such that the lattice point $v = \sum_i c_i w^{M_i}$ is a convex combination of weight vectors. By Proposition 5.4 there is an edge label τ on the boundary in the first and last square of $G_{T,\lambda}$ that occurs exactly twice in $G_{T,\lambda}$. Any ρ -symmetric matching must either include or not include both edges labeled τ , so $(w^{M_i})_\tau$ is 0 or 1 for all M_i (recall the definition of $\overline{\text{wt}}(M)$). Since v is an integer, either all M_i include both edges labeled τ or none of them do.

Arguing as in the proof of Lemma 5.2, the edges in M_i are determined from the first square to the next non-corner square on both ends of $G_{T,\lambda}$. Removing those squares from $G_{T,\lambda}$ yields a strictly smaller subgraph G' with ρ -symmetric matchings $\{M'_i\}_i$. Note that adding the same set of edges to each M'_i yields $\{M_i\}_i$, and $\sum_i c_i w^{M'_i}$ is a convex combination of weight vectors of G' equal to a lattice point. By Lemma 5.7, we can repeat this argument to remove tiles from both ends of $G_{T,\lambda}$ until we have G' containing no tiles from $G_{T,\rho,1}$ and $G_{T,\rho,2}$. Then the ρ -symmetry condition on G' is vacuous, so $P(G')$ is saturated by Lemma 5.7 and Proposition 5.8. Thus, $\sum_i c_i w^{M'_i} = w^{M_j}$ for one of the matchings M_j . And since $\{M'_i\}_i$ determines $\{M_i\}_i$ at each stage, we have $\sum_i c_i w^{M_i} = w^{M_j}$ as desired. \square

Proposition 5.8 and Proposition 5.9, together with Remarks 2.15, give the following result.

Theorem 5.10. *Let \mathcal{A}^{bd} be a type D cluster algebra with boundary coefficients. Then the Newton polytope of any cluster variable, written as a Laurent polynomial in an arbitrary seed, is saturated.*

Remark 5.11. Note that Theorem 5.10 does not hold for arbitrary surface-type cluster algebras with boundary coefficients; see Section 6.1.

Next, we classify when $N^{\text{bd}}(T, \gamma)$ is empty. The following simple lemma will be very handy.

Lemma 5.12. *Given $G_{T,\gamma}$, suppose there is an edge e with $\ell(e)$ unique. Then if there is a set of matchings S and a lattice point $\eta = \sum_{M \in S} c_M w^M$ with $\sum_{M \in S} c_M = 1$ and $c_M > 0$ for all $M \in S$, the coordinate $(w^M)_{\ell(e)}$ must be the same for all $M \in S$.*

Proof. Each $w_{\ell(e)}^M$ is either 0 or 1, depending on whether or not e was included in the perfect matching. Restricting the convex combination to the coordinate $\ell(e)$ yields a convex combination of 0s and 1s that is equal to an integer. Since each $c_M > 0$, this is only possible if it is a convex combination of only 0s or only 1s. \square

Now, we give three lemmas on emptiness and non-emptiness, which cover all Newton polytopes $N(T, \gamma)$.

Lemma 5.13. *Let T be an ideal triangulation of \mathbf{P}^\bullet . If γ is an arc that intersects each arc of T at most once, then $P(G_{T,\gamma})$ is empty.*

Proof. We will prove this by induction on the number of squares in $G_{T,\gamma}$. For the base case where there is a single square, there is some edge e with $\ell(e)$ unique. Given a set of matchings S as in Lemma 5.12, that lemma implies that either $e \in M$ or $e \notin M$ for all $M \in S$. So $|S| = 1$, implying emptiness.

Next, suppose $P(G_{T,\gamma})$ is empty for all $G_{T,\gamma}$ with at most t boxes. Suppose there is an arc τ such that $G_{T,\tau}$ has $t + 1$ boxes, and suppose there exists a set of matchings S as in Lemma 5.12. By Lemma 5.4, there is a square α at an end of $G_{T,\tau}$ and a boundary edge $e \in \alpha$ with $\ell(\alpha)$ unique in $G_{T,\tau}$. By Lemma 5.12, $M|_\alpha$ is the same for all $M \in S$. Let τ' be an arc such that $G_{T,\tau'}$ is equal to $G_{T,\tau}$ with α removed (the pathological boxed case of 5.6 is excluded by the hypothesis of this lemma). Letting a, b, d be the three boundary edges of α as in Figure 4.1, for each $M \in S$ define the matching M' of $G_{T,\tau'}$ as follows: if $a \in M$ for all $M \in S$, then $M' = M \setminus \{a\}$; otherwise $M' = M \cup \{c\} \setminus \{b, d\}$. Since $\sum_{M \in S} c_M w^{M'}$ is a lattice point, the inductive hypothesis implies $|S| = 1$, so $P(G_{T,\tau})$ is empty. \square

Lemma 5.14. *Let T be an ideal triangulation of \mathbf{P}^\bullet . If γ is a notched arc, then $P(G_{T,\gamma})$ is empty.*

Proof. Consider T as an ideal triangulation. If $k = 1$, by Remark 2.17 it suffices to show that $P(G_{T,\gamma^0})$ is empty, which follows from Lemma 5.13.

If $k > 1$, let λ be the loop enclosing γ and let ρ be the plain radius. If λ intersects each arc of T at most once, the γ -symmetry condition is vacuous and $P(G_{T,\gamma})$ is empty by Lemma 5.13. Thus, we assume that λ intersects at least one arc more than once, without loss of generality including ε_1 .

Let α and α' be the isomorphic squares on the ends of $G_{T,\rho,1}$ and $G_{T,\rho,2}$ respectively. By Lemma 5.4 we have boundary edges with $e \in \alpha$ and $e' \in \alpha'$ such that $\ell(e) = \ell(e')$ does not label any other edges in $G_{T,\gamma}$. Either $e, e' \in M$ or $e, e' \notin M$ for any γ -symmetric matching M . Letting G' be the snake graph obtained by removing α, α' from $G_{T,\gamma}$, we can use the method of Lemma 5.13 simultaneously on both ends to reduce any set of matchings of $G_{T,\gamma}$ satisfying the hypothesis of Lemma 5.12 to a set of matchings on G' satisfying the same hypothesis.

If λ intersects at least 2 non-radius arcs of T , then $G' = G_{T,\lambda'}$ where λ' is a loop with both endpoints moved as shown in Figure 5.6, and λ' intersects one fewer arc of T . However, if λ intersects only ε_1 and radii of T , then we find ourselves in the pathological boxed case; the γ -symmetry condition is vacuous for G' , so we directly show $P(G')$ is empty for such G' . Let $\sum_{M \in S} c_M \bar{w}^M$ satisfy the hypothesis of Lemma 5.12. Then each of $\varepsilon_2, \dots, \varepsilon_k$ is contained in all of or none of $M \in S$, since they each label a unique edge. If at least one of these is included, then each $M \in S$ is uniquely determined; if none of the interior edges of G' are included, then there are two possible matchings $M \in S$ but they have the same matching vector. Thus, $|S| = 1$, proving that $P(G')$ is empty. \square

Lemma 5.15. *Let T be an ideal triangulation of \mathbf{P}^\bullet . If $\gamma \notin T$ is a plain arc intersecting some arc of T more than once, then $P(G_{T,\gamma})$ is not empty.*

Proof. Without loss of generality, γ intersects ε_1 twice. If $k > 1$, then the squares corresponding to ρ_1 and ρ_k are non-corner squares, so there is a matching that includes a pair of opposite edges of each of the two squares labeled ε_1 . There are four choices of which pair is chosen from each square, leaving the rest of the matching the same. These four matchings yield three matching vectors, one of which is the midpoint of the other two, so $P(G_{T,\gamma})$ is not empty.

If $k = 1$, then there are four matchings of the three tiles labeled $\rho_1, \varepsilon_1, \rho_1$ (see Figure 5.8) again with three distinct matching vectors with one the midpoint of the other two, and these four matchings can be extended identically to the rest of the diagram to show that $P(G_{T,\gamma})$ is not empty. \square

Combining these lemmas yields the desired classification.

Theorem 5.16. *Let \mathcal{A}^{bd} be a type D cluster algebra with boundary冻 at seed Σ , corresponding to a tagged triangulation T . Let γ be a tagged arc and let $N^{\text{bd}}(T, \gamma)$ be the Newton polytope of x_γ , written as a Laurent polynomial in Σ .*

- *If γ is plain and $T \neq T^p$, then $N^{\text{bd}}(T, \gamma)$ is empty if and only if γ intersects no arc of T more than once.*
- *If γ is plain and $T = T^p$, then $N^{\text{bd}}(T, \gamma)$ is empty if and only if γ intersects no arc of T° more than once.*
- *If γ is notched, then $N^{\text{bd}}(T, \gamma)$ is empty.*

Proof. If T has all radii plain, then $T \neq T^p$ and T corresponds to an ideal triangulation T' . As before, we use Lemma 3.4 to note that emptiness of $N^{\text{bd}}(T, \gamma)$ is equivalent to emptiness of $P^{\text{bd}}(G_{T',\gamma})$. By Lemma 5.13, Lemma 5.14, and Lemma 5.15, the stated condition is a precise characterization of emptiness of $P(G_{T',\gamma})$.

If T has all radii notched, then $T \neq T^p$ and T^p corresponds to an ideal triangulation T' . If γ is not a radius, then by Remark 2.17 emptiness of $N^{\text{bd}}(T, \gamma)$ is equivalent to emptiness of $P^{\text{bd}}(G_{T',\gamma})$, and we can proceed as above. If γ is a radius, then emptiness of $N^{\text{bd}}(T, \gamma)$ is equivalent to emptiness of $P^{\text{bd}}(G_{T',\gamma^p})$, and the latter is always empty.

Finally, if T has a notched and un-notched radius ρ, ρ^\bowtie , then $T = T^p$ and T corresponds to an ideal triangulation $T' = T^\circ$ replacing ρ^\bowtie with a loop λ . Emptiness of $N^{\text{bd}}(T, \gamma)$ is equivalent to emptiness of $P^{\text{bd}}(T^\circ, \gamma)$ by Lemma 3.4, and the latter is only non-empty if γ intersects some arc of T° more than once. \square

5.2. Principal coefficients

As with Type A, the results for Type D with principal coefficients are very similar to those with boundary frozen variables. In this section, let $\pi = \pi^{\text{pc}}$.

Having developed the machinery of the principal perfect matching polytope, the proofs are almost identical to the boundary coefficients case. But first we need one lemma about the structure of the principal coefficient variables in Type D:

Lemma 5.17. *For T an ideal triangulation of \mathbf{P}^\bullet and γ a loop, the bottom matching of $G_{T,\gamma}$ is γ -symmetric.*

Proof. If γ only intersects radii, then the γ -symmetry condition holds vacuously. If γ intersects a single non-radius arc of T , then $G_{T,\gamma}$ looks like Figure 5.4. The bottom matching includes two boundary edges from one end square and one boundary edge from the other, which is γ -symmetric. If γ intersects more non-radius arcs of T , then $G_{T,\gamma}$ will look like Figure 5.4 extended on both ends with isomorphic squares, and we see inductively that the bottom matching is always γ -symmetric. \square

We will now state the results and note how the proofs differ from the boundary coefficients case.

Theorem 5.18. *Let \mathcal{A}^{pc} be a type D cluster algebra with principal coefficients at a seed Σ . Then the Newton polytope of any cluster variable, written as a Laurent polynomial in Σ , is saturated.*

Proof. As usual, we may assume that $\Sigma = \Sigma_{T'}$ where T' is a tagged triangulation corresponding to an ideal triangulation T .

To prove Lemma 5.2 for principal coefficients, note that if the first square α of $G_{T,\gamma}$ has an edge with a unique label, then no other square of $G_{T,\gamma}$ is labeled $\ell(\alpha)$. Therefore, all $\bar{v} = (\bar{v}_1, \bar{v}_2) \in \bar{P}^{\text{pc}}(G_{T,\gamma})$ satisfy $(\bar{v}_2)_{\ell(\alpha)} = (\pi(\bar{v})_2)_{\ell(\alpha)}$. Then for any lattice point $\eta \in P^{\text{pc}}(G_{T,\gamma})$, each $\bar{\eta} \in \pi^{-1}(\eta)$ has $(\bar{\eta}_2)_{\ell(\alpha)} \in \mathbb{Z}$. By Corollary 3.6, each $\bar{v} \in \bar{P}^{\text{pc}}(G_{T,\gamma})$ has $(\bar{v}_2)_{\ell(\alpha)} = (\bar{v}_1)_{\ell(e)}$ for some edge e of α . Therefore, $(\bar{v}_1)_{\ell(e)}$ is an integer, and we can proceed exactly as in Lemma 5.2 to extend a matching of a smaller saturated snake graph to a matching with weight vector $\pi(\bar{v})$.

Likewise we can prove the analogue of Lemma 5.3. If two isomorphic squares α, α' at the ends of $G_{T,\gamma}$ have corresponding edges $e \in \alpha, e' \in \alpha'$ with $\ell(e) = \ell(e')$ labeling no other edges, then there are no other squares labeled by $\ell(\alpha) = \ell(\alpha')$. Exactly as above, we can convert equations in the coordinates of \bar{v}_2 into equations involving coordinates of \bar{v}_1 , and then apply the proof of Lemma 5.3 to construct a matching with weight vector $\pi(\bar{v})$.

For Lemma 5.5, since the squares of G' are distinct, the coordinates of \bar{v}_2 must be 0 or 1, so $(\bar{v}_1)_e$ must be an integer for all boundary edges e of G' . Then the same must be true for interior edges e of G' , showing that $\pi(\bar{v})$ is the weight vector of a matching.

For Lemma 5.6, for $k > 1$ we apply precisely the same reasoning to show that if α is a square of $G_{T,\gamma}$ with $\ell(\rho)$ a radius and e is an edge of α on the boundary of $G_{T,\gamma}$, then $(\bar{v}_1)_{\ell(e)}$ is 0 or 1 for all \bar{v} . Noting that the squares corresponding to ρ_1 and ρ_k are non-corner squares of $G_{T,\gamma}$, Corollary 3.6 implies that $(\bar{v}_1)_{\varepsilon_2}, \dots, (\bar{v}_1)_{\varepsilon_k}$ are each 0 or 1. Then casework shows that both $(\bar{v}_2)_{\varepsilon_1}$ and $(\bar{v}_2)_{\varepsilon'_1}$ must be integers too, so $\pi(\bar{v})$ corresponds to a matching. If $k = 1$, then $G_{T,\gamma}$ consists of three tiles, and we can check directly that no nontrivial convex combination of matching vectors yields a lattice point.

Lemma 5.4 and Lemma 5.7 can be applied directly to the principal coefficients case (using our work above for the latter), so we can put all of this together to replicate the proof of Lemma 5.8.

For Lemma 5.9, note that by Lemma 5.17 the coordinates $(v_2)_{\ell(\alpha)}$ corresponding to squares α in $G_{T,\gamma,1}$ and $G_{T,\gamma,2}$ determine each other by the γ -symmetry condition. Therefore, we can adapt the above arguments to $G_{T,\gamma,1}$ and $G_{T,\gamma,2}$ to induct simultaneously on both ends of $G_{T,\gamma}$, proceeding as in the previous case. \square

Remark 5.19. Many of the lemmas appearing in the above proof depend crucially on the combinatorics of snake graphs from punctured polygons. In particular, Lemmas 5.2 and 5.3, which give the essence of the inductive step, both assume that certain edge labels appear very few times. However, for snake graphs from other surfaces, we have much less control over how many times an edge label appears (see Figures 6.1, 6.2, and 6.3). This is the main obstacle in using similar techniques to prove saturation for cluster variables in arbitrary surface-type cluster algebras with principal coefficients.

Next, we characterize when Newton polytopes for type D cluster variables with principal coefficients are empty. As with the boundary frozens case, not all Newton polytopes are empty. Recall that if T is a tagged triangulation of \mathbf{P}^\bullet , T^p denotes the triangulation obtained by switching the tagging of each radius. Further, $T = T^p$ if and only if T corresponds to an ideal triangulation with a loop.

Theorem 5.20. *Let \mathcal{A}^{pc} be a type D cluster algebra with principal coefficients at a seed Σ , corresponding to a tagged triangulation T . Let γ be a tagged arc and let $N^{pc}(T, \gamma)$ be the Newton polytope of x_γ , written as a Laurent polynomial in Σ .*

- If γ is plain and $T \neq T^p$, then $N^{pc}(T, \gamma)$ is empty if and only if γ intersects no arc of T more than once.
- If γ is plain and $T = T^p$, then $N^{pc}(T, \gamma)$ is empty if and only if γ intersects at most one arc of T° more than once.
- If γ is notched, then $N^{pc}(T, \gamma)$ is empty.

Proof. First, consider the case that γ is plain. Note that Lemma 5.12 also applies to squares α of $G_{T, \gamma}$ with $\ell(s)$ unique.

As in our proof of Theorem 5.18, if the first square α of $G_{T, \gamma}$ has an edge e on the boundary of $G_{T, \gamma}$ with $\ell(e)$ unique, then $\ell(\alpha)$ is also unique. Then given a set of matchings S satisfying the hypothesis of Lemma 5.12, each of the three edges of α on the boundary of $G_{T, \gamma}$ are either included or excluded in all $e \in M$. So as in the proof of Lemma 5.13 we can reduce each $M \in S$ to a matching M' on a smaller snake graph, with $\sum_{M \in S} c_M \bar{w}_{pc}^{M'}$ equal to a lattice point.

If γ intersects each arc of T at most once, then we can use this method to reduce the snake graph until we have removed all squares, implying emptiness by induction. If T contains a loop that γ intersects twice, then we can reduce the snake graph to the three tiles corresponding to $\varepsilon_1, \rho_1, \varepsilon_1$. We saw in the proof of Theorem 5.18 that for matchings M of this graph, $\{\bar{w}_{pc}^M\}_M$ have no convex combination equal to a lattice point, proving emptiness.

Conversely, the construction of Lemma 5.15 also violates emptiness for principal coefficients if T has no loop and γ intersects some arc more than once. If T has a loop and γ intersects at least two arcs more than once, let τ be the arc intersected before/after the loop ε_1 . Then we can adapt the construction of Lemma 5.15 with τ instead of ε_1 , i.e., constructing the four matchings using pairs of opposite sides from each of the two squares corresponding to τ . These can all be extended identically to the rest of the snake graph, and one of the resulting principal matching vectors is the midpoint of two others.

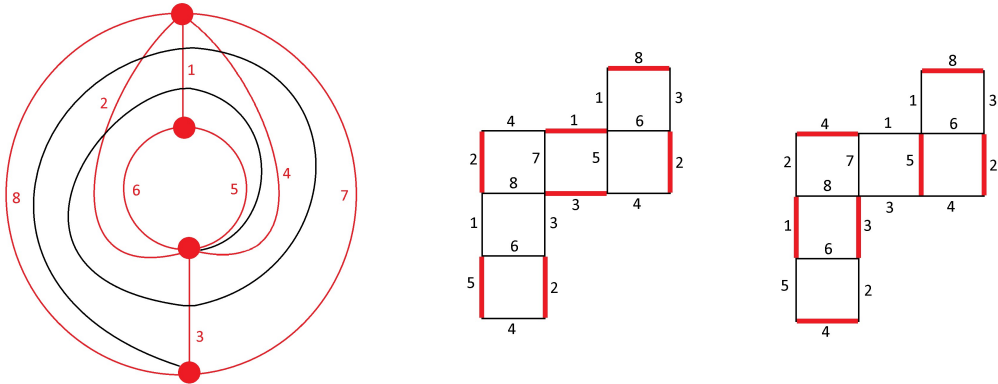


Figure 6.1: On the left is an arc τ (black) and a triangulation T of an annulus. On the right are two matchings of the snake graph $G_{T,\gamma}$. The midpoint of the weight vectors of these matchings does not correspond to a matching.

Now, let γ be notched. By Lemma 5.17, we can use the γ -symmetry condition to apply our work above to $G_{T,\gamma,1}$ and $G_{T,\gamma,2}$. Letting G' be $G_{T,\gamma}$ with isomorphic subgraphs removed from each end, we can reduce $\sum_{M \in S} c_M \bar{w}_{\text{pc}}^M$ with $M \in S$ matchings of $G_{T,\gamma}$ to $\sum_{M \in S} c_M \bar{w}_{\text{pc}}^{M'}$ with each M' a matching of G' . To finish proving this analogue of Lemma 5.14, letting G' consist only of squares labeled by radii, note that each square has a unique label. So if S satisfies the hypothesis of Lemma 5.12, then all matchings in S agree on the boundary edges of G' . And as we saw in the proof of Theorem 5.18, the boundary edges in a matching of G' determine the matching, proving emptiness. \square

Remark 5.21. It is possible to construct a pair of inverse affine maps $\overline{P}^{\text{pc}}(G_{T,\gamma}) \longleftrightarrow \overline{P}(G_{T,\gamma})$, proving that the polytopes are combinatorially equivalent. Furthermore, both maps take lattice points to lattice points. However, they do not descend to well-defined maps $P^{\text{pc}}(G_{T,\gamma}) \longleftrightarrow P(G_{T,\gamma})$, since affine maps do not commute with adding coordinates. Nevertheless, perhaps investigating these maps could be a fruitful avenue for future work.

6. Cluster variable Newton polytopes for other surfaces

Now, we examine cluster algebras from surfaces other than \mathbf{P} and \mathbf{P}^\bullet . We will not define them here, but similar snake graph expansion formulas hold for cluster variables, see [MSW11].

Types A and D are the only cluster algebras from surfaces that are finite type, and are in general unusually well-behaved from a combinatorial perspective. This holds for Newton polytopes of cluster variables as well. Many of the results in the previous sections fail for arbitrary cluster algebras from surfaces.

6.1. Counterexamples

We give some examples demonstrating that saturation does not hold in general for cluster algebras from surfaces with boundary frozen variables.

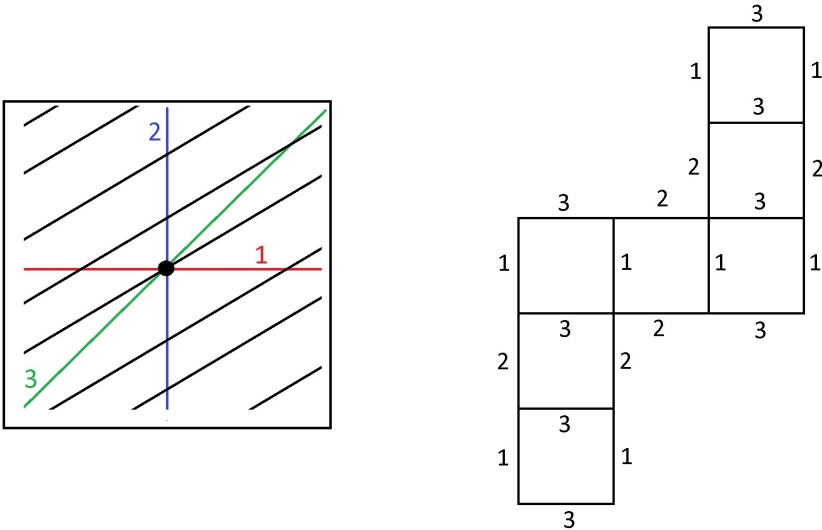


Figure 6.2: On the left is an arc γ (black) and a triangulation T of a punctured torus. On the right is the snake graph $G_{T,\gamma}$.

Example 6.1 (Annulus). For an annulus with two marked points on each boundary component, let triangulation T and arc γ be as shown in Figure 6.1 on the left. The matchings of $G_{T,\gamma}$ on the right yield weight vectors $(1, 3, 1, 0, 1, 0, 0, 1)$ and $(1, 1, 1, 2, 1, 0, 0, 1)$. Their midpoint, $(1, 2, 1, 1, 1, 0, 0, 1)$, does not correspond to a matching. Thus, $P(G_{T,\gamma})$ is not saturated.

Example 6.2 (Punctured Torus). For a torus with one marked point in the interior, let triangulation T and arc γ be as shown in Figure 6.2. For $G_{T,\gamma}$, shown on the right, one can check that each matching will include an even number of edges with each label. But there are pairs of weight vectors whose midpoints have odd coordinates (e.g., let one matching include two opposite sides of one square, and let the other matching be the same but with the other two sides of that square), so these midpoints cannot correspond to matchings. Thus, $P(G_{T,\gamma})$ is not saturated.

Example 6.3 (Twice Punctured Torus). For a torus with two marked points in the interior, let triangulation T and arc γ be as shown in Figure 6.3 on the left. The matchings of $G_{T,\gamma}$ on the right yield weight vectors $(2, 0, 1, 1, 1, 2)$ and $(0, 2, 1, 1, 1, 2)$. Their midpoint, $(1, 1, 1, 1, 1, 2)$, does not correspond to a matching. Thus, $P(G_{T,\gamma})$ is not saturated.

These examples were computed using a combination of original Python code (available upon request) and the online Polymake software.

Remark 6.4. We remark that the above examples do not contradict Conjecture 1.2. However, note that none of the snake graphs in Figures 6.1, 6.2, and 6.3 fulfill the hypotheses of Lemmas 5.2 and 5.3. This indicates that an inductive proof of Conjecture 1.2 would have a substantially more intricate inductive step.

6.2. Conjectures

Given these counterexamples and the exceptionalness of finite type cluster algebras, we conjecture the following.

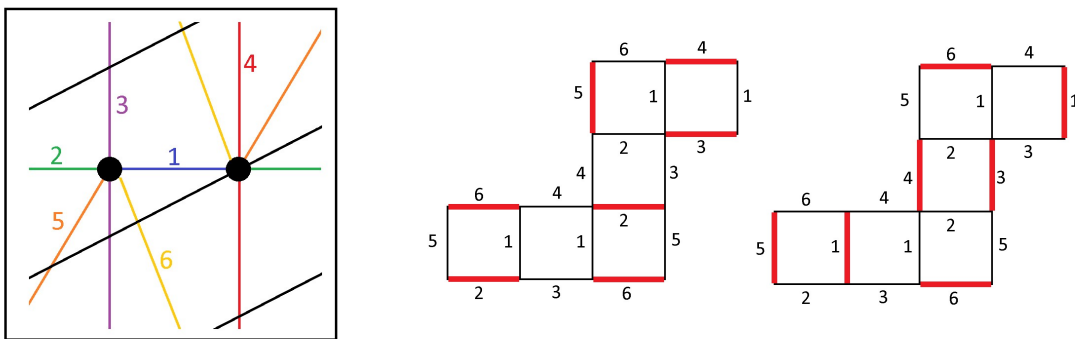


Figure 6.3: On the left is an arc γ (black) and a triangulation T of a twice-punctured torus. On the right are two matchings of the snake graph $G_{T,\gamma}$. The midpoint of the weight vectors of these matchings does not correspond to a matching.

Conjecture 6.5. Let \mathcal{A}^{bd} be a cluster algebra from a surface (S, M) with boundary frozen variables. Then $N^{\text{bd}}(T, \gamma)$ is saturated for all T, γ only if (S, M) is \mathbf{P} or \mathbf{P}^\bullet .

Noting that our proofs in types A and D made use of certain labels appearing at most once or twice in $G_{T,\gamma}$, perhaps saturation fails when snake graphs get too big and labels repeat arbitrarily many times — which can always occur in non-finite type cluster algebras from surfaces. Thus, we have a stronger version of Conjecture 6.5.

Conjecture 6.6. Let \mathcal{A}^{bd} be a cluster algebra from a surface (S, M) with boundary frozen variables. There exists $B \in \mathbb{N}$ such that if $G_{T, \gamma}$ has more than B squares, then $N^{\text{bd}}(T, \gamma)$ is not saturated.

Note that Conjecture 6.6 is vacuously true if (S, M) is \mathbf{P} or \mathbf{P}^\bullet since the number of squares in $G_{T, \gamma}$ is bounded in these finite type cases.

We note that we have not found a counterexample to Fei's conjecture: that cluster variable Newton polytopes in cluster algebras with principal coefficients are saturated.

Acknowledgements

Both authors would like to thank Lauren Williams for helping to steer this research.

References

[AHHL20] Nima Arkani-Hamed, Song He, and Thomas Lam. Cluster configuration spaces of finite type. 2020. arXiv:2005.11419.

[BK00] Imre Bárány and Jean-Michel Kantor. On the number of lattice free polytopes. *European J. Combin.*, 21(1):103–110, 2000. Combinatorics of polytopes. doi: 10.1006/eujc.1999.0324.

- [CGM⁺17] Man Wai Cheung, Mark Gross, Greg Muller, Gregg Musiker, Dylan Rupel, Salvatore Stella, and Harold Williams. The greedy basis equals the theta basis: a rank two haiku. *J. Combin. Theory Ser. A*, 145:150–171, 2017. doi:10.1016/j.jcta.2016.08.004.
- [DO95] M. Deza and S. Onn. Lattice-free polytopes and their diameter. *Discrete Comput. Geom.*, 13(1):59–75, 1995. doi:10.1007/BF02574028.
- [Edm65] Jack Edmonds. Paths, trees, and flowers. *Canadian J. Math.*, 17:449–467, 1965. doi:10.4153/CJM-1965-045-4.
- [Fei19] Jiarui Fei. Combinatorics of F-polynomials. 2019. arXiv:1909.10151.
- [FST08] Sergey Fomin, Michael Shapiro, and Dylan Thurston. Cluster algebras and triangulated surfaces. I. Cluster complexes. *Acta Math.*, 201(1):83–146, 2008. doi:10.1007/s11511-008-0030-7.
- [FZ02] Sergey Fomin and Andrei Zelevinsky. Cluster algebras. I. Foundations. *J. Amer. Math. Soc.*, 15(2):497–529, 2002. doi:10.1090/S0894-0347-01-00385-X.
- [FZ03] Sergey Fomin and Andrei Zelevinsky. Cluster algebras. II. Finite type classification. *Invent. Math.*, 154(1):63–121, 2003.
- [FZ07] Sergey Fomin and Andrei Zelevinsky. Cluster algebras. IV. Coefficients. *Compos. Math.*, 143(1):112–164, 2007. doi:10.1112/S0010437X06002521.
- [GHKK18] Mark Gross, Paul Hacking, Sean Keel, and Maxim Kontsevich. Canonical bases for cluster algebras. *J. Amer. Math. Soc.*, 31(2):497–608, 2018. doi:10.1090/jams/890.
- [JLS20] Dennis Jahn, Robert Löwe, and Christian Stump. Minkowski decompositions for generalized associahedra of acyclic type. 2020. arXiv:2005.14065.
- [Kal13] Adam Kalman. Newton polytopes of cluster variables of type A_n . 2013. arXiv:1310.0555.
- [Kan99] Jean-Michel Kantor. On the width of lattice-free simplices. *Compositio Math.*, 118(3):235–241, 1999. doi:10.1023/A:1001164317215.
- [LLS20] Kyungyong Lee, Li Li, and Ralf Schiffler. Newton polytopes of rank 3 cluster variables. 2020. arXiv:1910.14372.
- [LLZ14] Kyungyong Lee, Li Li, and Andrei Zelevinsky. Greedy elements in rank 2 cluster algebras. *Selecta Math. (N.S.)*, 20(1):57–82, 2014. doi:10.1007/s00029-012-0115-1.
- [LP86] L. Lovász and M. D. Plummer. *Matching theory*, volume 121 of *North-Holland Mathematics Studies*. North-Holland Publishing Co., Amsterdam; North-Holland Publishing Co., Amsterdam, 1986. Annals of Discrete Mathematics, 29.
- [LP22] Fang Li and Jie Pan. Recurrence formula, positivity and polytope basis in cluster algebras via newton polytopes. 2022. arXiv:2201.01440.
- [MSW11] Gregg Musiker, Ralf Schiffler, and Lauren Williams. Positivity for cluster algebras from surfaces. *Adv. Math.*, 227(6):2241–2308, 2011. doi:10.1016/j.aim.2011.04.018.

- [MSW13] Gregg Musiker, Ralf Schiffler, and Lauren Williams. Bases for cluster algebras from surfaces. *Compos. Math.*, 149(2):217–263, 2013. doi:10.1112/S0010437X12000450.
- [MTY19] Cara Monical, Neriman Tokcan, and Alexander Yong. Newton polytopes in algebraic combinatorics. *Selecta Math. (N.S.)*, 25(5):Paper No. 66, 37, 2019. doi:10.1007/s00029-019-0513-8.
- [SW05] David Speyer and Lauren Williams. The tropical totally positive Grassmannian. *J. Algebraic Combin.*, 22(2):189–210, 2005. doi:10.1007/s10801-005-2513-3.
- [SZ04] Paul Sherman and Andrei Zelevinsky. Positivity and canonical bases in rank 2 cluster algebras of finite and affine types. *Mosc. Math. J.*, 4(4):947–974, 982, 2004. doi:10.17323/1609-4514-2004-4-4-947-974.